



University
of Glasgow

<https://theses.gla.ac.uk/>

Theses Digitisation:

<https://www.gla.ac.uk/myglasgow/research/enlighten/theses/digitisation/>

This is a digitised version of the original print thesis.

Copyright and moral rights for this work are retained by the author

A copy can be downloaded for personal non-commercial research or study,
without prior permission or charge

This work cannot be reproduced or quoted extensively from without first
obtaining permission in writing from the author

The content must not be changed in any way or sold commercially in any
format or medium without the formal permission of the author

When referring to this work, full bibliographic details including the author,
title, awarding institution and date of the thesis must be given

Enlighten: Theses

<https://theses.gla.ac.uk/>
research-enlighten@glasgow.ac.uk

LATTICE VACANCIES AND DIFFUSION IN THE
GOLD-NICKEL ALLOY SYSTEM.

by

A.F. CRAWLEY, B.Sc., A.R.C.S.T.

Thesis submitted to the University of Glasgow
for the degree of Doctor of Philosophy.

April, 1965.

ProQuest Number: 10646049

All rights reserved

INFORMATION TO ALL USERS

The quality of this reproduction is dependent upon the quality of the copy submitted.

In the unlikely event that the author did not send a complete manuscript and there are missing pages, these will be noted. Also, if material had to be removed, a note will indicate the deletion.



ProQuest 10646049

Published by ProQuest LLC (2017). Copyright of the Dissertation is held by the Author.

All rights reserved.

This work is protected against unauthorized copying under Title 17, United States Code
Microform Edition © ProQuest LLC.

ProQuest LLC.
789 East Eisenhower Parkway
P.O. Box 1346
Ann Arbor, MI 48106 – 1346

SUMMARY

The gold-nickel alloy system has been studied from two aspects:

1. Lattice parameters and densities at 900°C.
2. Diffusion of gold into nickel.

It has been previously reported that this system displayed some anomolous deviations in the lattice parameter and density values arising from a concentration at certain compositions of vacant lattice sites which was far in excess of that required for thermal equilibrium. These anomalies were attributed to lattice strain energy considerations in the region of Brillouin zone overlaps. The present work gave no evidence to support this view, there being no deviations in the lattice parameter and density results.

The intrinsic diffusion coefficients D^* of gold in nickel at several temperatures have been determined using the instantaneous source solution to Fick's Second Law for unidimensional diffusion. Penetration curves obtained by radioactivation analysis did, however, point to a higher gold concentration than had been expected at depths beyond the immediate surface layers. These discrepancies with earlier diffusion results are discussed under the following headings:-

- (a) Experimental errors in the method of determining the depth of penetration.
- (b) The possibility of an excess of grain boundary diffusion relative to volume diffusion.

(c) The validity of applying the solution to Fick's Second Law in the present case.

Studies of the diffusion of gold into a single crystal of nickel helped to elucidate the relevance of these factors.

C O N T E N T S

PART I.

LATTICE VACANCIES IN THE GOLD-NICKEL ALLOY SYSTEM.

	<u>PAGE</u>
<u>Introduction:</u>	1.
 <u>Chapter 1 - Theory of Alloy Formation</u>	
1. Factors affecting alloy formation.	3.
2. The gold-nickel alloy system.	9.
3. Vacant lattice sites.	16.
 <u>Chapter 2 - Analytical techniques.</u>	
1. X-ray analysis of a crystal lattice.	22.
2. Analysis of gold by cupellation.	30.
 <u>Chapter 3 - Experimental procedure.</u>	
1. Preparation and annealing of gold-nickel alloys-1.	31.
2. Preparation and annealing of gold-nickel alloys-2.	37.
3. Preparation and heat treatment of x-ray powder specimens.	3
4. Determination of lattice parameters.	39.
5. Determination of densities.	41.
 <u>Chapter 4 - Results.</u>	
1. Lattice parameters of gold-nickel alloys-1.	47
2. Lattice parameters of gold-nickel alloys-2.	50
3. Densities of gold-nickel alloys.	51
4. Composition of the alloys.	53
 <u>Chapter 5 - Discussion.</u>	57

PART II

SELF-DIFFUSION OF GOLD IN NICKEL.

	<u>PAGE.</u>
<u>Introduction:</u>	61.
 <u>Chapter 1. - Theory of diffusion in metals</u>	
1. Mathematics of diffusion.	63.
2. Mechanisms of diffusion.	70.
3. Atomic theory of diffusion.	73.
4. Grain boundary and volume diffusion.	79.
 <u>Chapter 2 - Analytical techniques.</u>	
1. Radioactivation analysis.	81.
2. Gamma scintillation spectrometry.	85.
 <u>Chapter 3 - Experimental procedure.</u>	
1. Deposition of a thin film of gold.	87.
2. Electrolytic polishing of nickel.	92.
3. Diffusion anneals.	94.
4. Determination of the penetration curve.	97.
5. Preparation of single crystals.	102.
 <u>Chapter 4 - Results and discussion.</u>	106.
 <u>CONCLUSION</u>	115.

INTRODUCTION

The gold-nickel system has attracted the attention of many investigators on account principally of the large immiscibility gap which the system displays. This feature points to a great lattice strain in the solid solution phase which exists at all compositions above the immiscibility gap. Both practical and theoretical thermodynamic studies have been performed to shed some light on the distortional energy of the solid solution phase.

Some evidence has appeared in the literature of the presence in the system of vacant lattice sites manifested by discontinuities in the variation of lattice spacings with compositions and by marked differences between the theoretical and the measured densities. These excess vacancies have been attributed to Brillouin Zone effects. There has been some disagreement on this aspect and consequently a further investigation of the lattice dimensions seemed necessary.

As an extension of a vacancy investigation diffusion studies would be enlightening since it is generally accepted that diffusion in the solid state occurs by way of vacant sites. The presence in any solid phase of vacancies in

excess of that required for thermal equilibrium would have been expected to cause enhanced rates of diffusion directly opposite in effect to the reduction in diffusion rates displayed by a phase under pressure when, in accordance with the principle of Le Chatelier, the equilibrium concentration of vacancies decreases.

It was, therefore, hoped that the present investigation of the gold-nickel system would offer some contribution to the Brillouin Zone Theory of Metals and to the theory of diffusion in the solid state.

PART I

LATTICE VACANCIES IN THE GOLD-NICKEL ALLOY SYSTEM

CHAPTER I

THEORY OF ALLOY FORMATION

SECTION 1.

FACTORS AFFECTING ALLOY FORMATION

The degree of substitutional solid solution in metallic phases has been shown by experimental observation to be governed by certain physical factors. For the most part, the efforts which have been made to systematise the likelihood and extent of solid solution formation have been studies of the alloys of the univalent and electronically relatively simple metals copper, silver and gold. Hume-Rothery has separated the effects of four physical factors ordained by solute and solvent which influence the structure and properties of solid solutions.

- (1) Atomic size difference.
- (2) Difference in electrochemical character.
- (3) Relative valency effect.
- (4) Electron concentration of valence electrons.

It is unjustifiable to apply the findings for the univalent metals to other systems but they serve to illustrate the types of limitation involved.

In the absence of a temperature dependent phase change, an increase in temperature will increase the degree of solid solution formation or allow the formation of solid solutions at regions above the areas of eutectoid, peritectoid and immiscibility. Such alterations in the extent of miscibility are allowed by the increased vibrational entropy of the system which allows the retention of solid solution despite the inhibiting effects of the above factors.

(1) The formation of a solid solution between atoms of disparate sizes causes lattice strain which consists of local lattice distortions, expansion or contraction of the lattice and a general upsetting of the periodicity of the lattice, all of which increases the internal energy of the system. Hume-Rothery from evidence gathered on alloys of copper, silver and gold with elements of the B sub-groups has shown that considerable solid solution may be formed provided that the difference in atomic diameters of the metals, given by the closest distance of approach of atoms in the pure metals, does not exceed 14-15%.

(2) Any system, metallic or otherwise, is in a state of maximum stability when its Gibbs free energy is at a minimum, and the system will tend under the restrictions of kinetics to

attain a state of minimum free energy. For metals which differ considerably in electrochemical character this minimum can be achieved by compound formation. Despite the presence of a favourable size factor, the ionic interactions between solute and solvent atoms hinder solid solution formation by causing the creation of the combined state.

(3) & (4) To evaluate the effects of these factors it is necessary to examine the fundamental concepts of the electron theory of metals. When atoms are brought together to form a metal, atomic interactions occur which cause the valence electrons to lose their discrete electronic energies and enter an electron band which extends over a certain energy range. The electron states of the free atoms become a series of energy states regions which are separated by ranges of forbidden energies. To display the distribution of the energy states of the electrons within each region, an $N(E)$ curve or density of states curve is used. The $N(E)$ curve is a representation of the number of quantum states in a particular energy range. By definition, the density of states is $N(E)$, where $N(E) dE$ is number of states per unit volume of crystal with energies in the range between E and $(E + dE)$. The manner of distribution of the energy states offers evidence of the internal electronic energy of the crystal.

For example, if a large number of states are available at low energy value, the structure will be electronically more stable than one which has a few energy states at high energy values. Density of states curves are shown in fig. 1 where:-

(a) There is a forbidden energy range EG between the most energetic electrons of the first range and the least energetic of the second range.

(b) There is an overlap of the ranges caused by the least energetic electrons of the second region occupying a lower energy state than the most energetic of the first region.

The first, second etc. ranges of energy of the energy states are referred to as the distribution of energy states in the first, second etc. Brillouin zone. A Brillouin zone is a graphical illustration of the energy states of an electron gas in k space or wave number space where $k = \frac{2\pi}{\lambda}$

(λ = wave length of the electron), and where the electrons in the highest energy states are on a surface termed the Fermi surface.

In essence, an alloy will assume a crystal structure which allows the electrons to occupy states of lowest energies. After the peak A of the N(E) curve, large energies are required to fill the remaining states. To avoid this energy expenditure, the structure may alter to one which has a higher peak at a higher energy thus allowing more energy states to be filled at lower energies

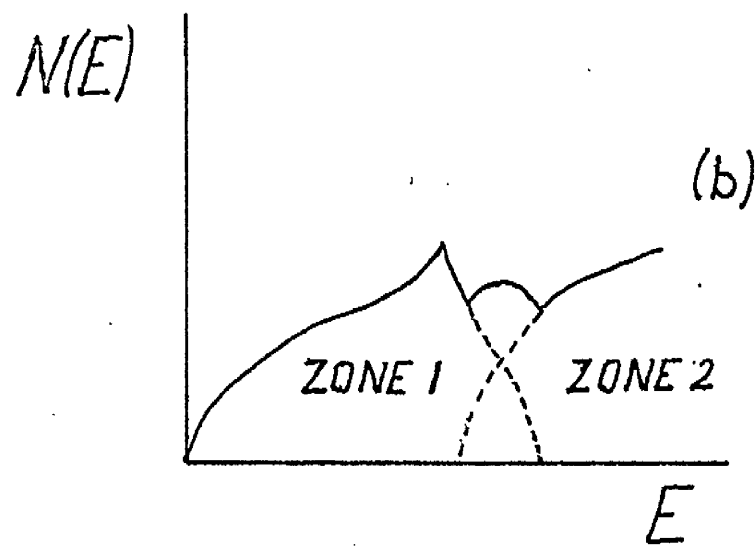
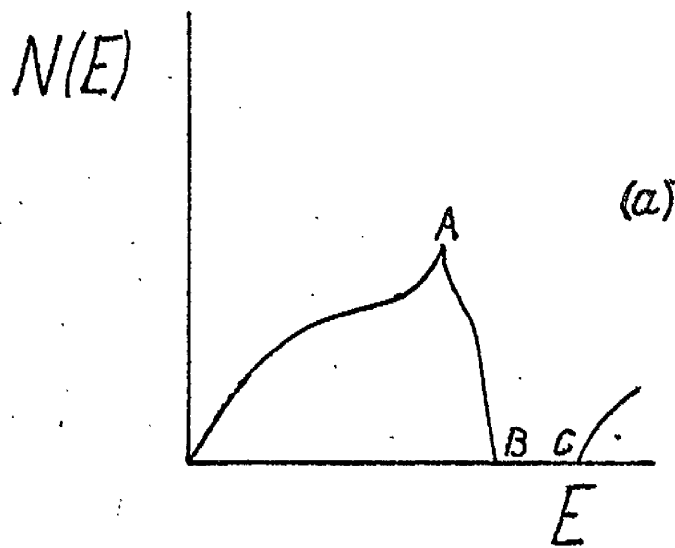


Fig 1. Density of States Curves

prior to the higher peak. The fundamental parameter of the electron theory is number of electrons per unit cell or if all lattice sites are occupied the electron to atom ratio is equivalent to this parameter. Hume-Rothery has proposed that the above energy considerations can explain the occurrence of electron compounds in alloys of copper, silver and gold where the $\alpha \longrightarrow \beta$ phase transformation occurs at an e/a of 3:2 and $\beta \longrightarrow \gamma$ at an e/a of 21 : 13.

The theory also suggests that when Brillouin Zone overlaps occur, that to avoid energetically expensive fillings of states just prior to overlapping, the structure may delay the process by removing atoms from occupied lattice sites to create vacant sites. In this way, the alloying addition of atoms of higher valency continues while the electron to atom ratio remains constant whereas the electrons per unit cell varies.

ORDERED STRUCTURES

From elementary energy considerations it is evident that a completely random solid solution of two metals is a state of maximum strain. A crystal lattice will, therefore, tend towards a state whereby the internal stress may be reduced. This effect can be achieved by ordering. A state of order exists when atoms show a preference for unlike neighbours. Long range order exists when nearest neighbours are dissimilar

throughout the entire crystal. To achieve this state as in the copper-gold system, the atoms take up new positions such that each atom is surrounded by unlike neighbours. The consequent relaxation of strain renders the structure very stable. Short range order exists when atoms show a preference for unlike neighbours over short distances of the atomic array.

SECTION 2.THE GOLD-NICKEL ALLOY SYSTEM.

The phase diagram of the gold-nickel system is shown in Fig. 2. A flat minimum occurs ^{in the liquidus and solidus curves.} in the system at 42 atomic per cent of nickel at 950°C. The form of the liquidus curve was established by the graphical interpolation of the results of several authors. ¹⁻⁴ Initially, ^{1,2} it was believed that a eutectic ^{was formed} between gold-rich and nickel-rich solid solutions. It was, however, later pointed out that at higher temperatures there was a continuous series of solid solutions. The determination of the solidus curve by Fraenkel ⁵ and Stern differed considerably from that by Hafner. ⁴ Fraenkel and Stern ⁵ from heating curves deduced higher values than did Hafner from cooling curves. Such a contingency is difficult to comprehend since values obtained from cooling curves are usually lower than those obtained from heating curves. No studies have been reported to clarify this anomaly, although most modern workers tend to favour the values given by Fraenkel and Stern. ⁵

A miscibility gap with a critical point was first reported by Fraenkel and Stern. ⁵ Several investigations ⁵⁻⁹ have been made into the form of the miscibility gap. The present

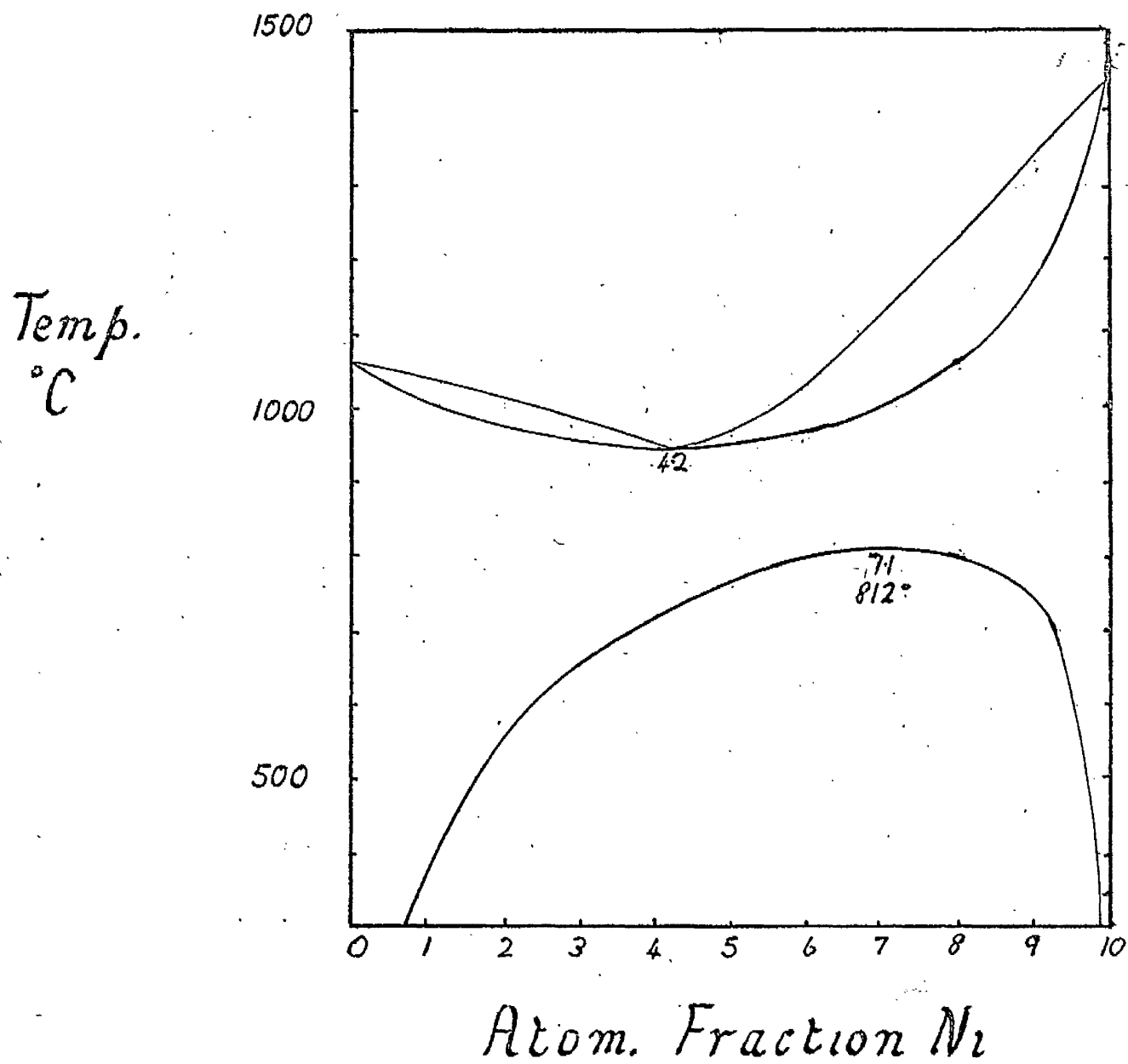


Fig. 2. Gold-Nickel System.

form as shown in fig.2 has been deduced from the work of Koster and Dannohl⁶ and Munster and Sagol⁷. Fourteen alloys between 27 and 88.5 at.% nickel were used by the latter to determine by resistivity measurements the shape of the miscibility gap. Their results follow a very smooth boundary which fits very neatly into an extrapolation of the curves at gold-rich and nickel-rich ends as determined by Koster and Dannohl⁶. Previous data for the miscibility gap by Fraenkel and Stern⁵ and Grube and Vaupel⁸ (who admitted that their results might be too high) do not give the same smooth continuity as those of Munster and Sagol⁷. An investigation by Gerlach⁹ did not yield the same continuous smooth curve although several of his points do correspond with the other studies. Hence, it may be asserted that the correct form of the miscibility gap is that shown in fig 2, having a peak at 812°C and 71 at.% nickel.

The presence of the miscibility gap and hence the implied instability of the *solid* solution phase has rendered the gold-nickel system to be of interest for thermodynamic study. Combined with the immiscibility effects, there are also the factors of a large difference in atomic ratio (1.44 $K_A Au$, 1.22 Ni) and the distinct differences in electronic structure which promotes some possible interaction between the 6s electron band of gold and the unfilled 3d band of nickel to form 5d hybridised bands.

Lattice parameters of gold-nickel alloys were first determined by Kubaschowski and Ebert¹⁰ in the course of a diffusion investigation but only three values are given.

//
 Ellwood and Bagley determined the lattice spacings and densities of alloys over the entire composition range but their results at the gold-rich end did not agree as closely as might have been expected with those of Kubaschowski and Ebert. Moreover, Ellwood and Bagley showed in their lattice parameter/composition curve certain anomalies which corresponded well with discrepancies between the theoretical and measured densities of their alloys. These discrepancies were attributed to vacant lattice sites.

¹²
 Day, in the course of a Thermodynamic investigation determined the lattice parameters of five alloys. He found that the curve of lattice parameter against composition was continuously smooth although his points are too widely dispersed to authoritatively criticize the previously reported form. However, his lattice parameter values do differ from those of Ellwood and Bagley and his density measurements do not manifest any discrepancies from the theoretical values.

¹²
 Day, whose lattice spacings are more¹⁰ in alignment with those of Kubaschowski and Ebert, did not state why these lattice parameters and density discrepancies differed from previous work.

A thermodynamic investigation was carried out
¹³
 by Siegle et al. Their results showed that the entropies
 of mixing (ΔS^{ms}) are almost twice those of ideal solutions
 and that the gold-nickel system showed a large positive deviation
 from Raoult's Law. They attributed the large positive enthalpies
 of solution to the lattice distortional energy which results
 from the large atomic size difference between gold and nickel.
 Calculations based on the heat of absorption arising solely
 through this lattice strain would more than account for the
 large positive enthalpy.
¹⁴
 Flinn et al. studied the local atomic
 arrangements in gold-nickel alloys by measurements of diffuse
 X-ray scattering and concluded that in the region of solid
 solution, the atoms displayed a preference for unlike neighbours
 (short range order). In the light of a quasi chemical theory
¹⁵
 such as that of Tagaki, which quantitatively predicts the average
 preference for like or unlike neighbours depending on whether
 or not the heats of mixing are positive or negative, this short
 range order was inconsistent with the positive heats of mixing
 but Flinn et al.
¹⁴
 argued that these large positive enthalpies
 arose from the lattice distortional energy which could be
 decreased by a relaxation of the structure through some degree
¹⁶
 of order. Averbach et al. continued the studies of Flinn
 et al in an attempt to corroborate the thermodynamic data

and the data on short range order.

¹⁷ Oriani investigated the heat capacity and entropy of a 0.517/0.483 gold/nickel alloy to estimate the vibrational contribution to the entropy of mixing which had been postulated by others and to obtain careful measurements of the deviation of the alloy from the Kopp-Neumann Rule which states that molar heats of alloys are obtained nearly additively from the atomic heats of the components i.e. for an alloy of x mole fraction A and y mole fraction B

$$\Delta C_p = C_{p_{AxBy}} - (xC_{p_A} + yC_{p_B})$$

That the gold-nickel system does not follow this rule is in keeping with the large positive enthalpies and entropies previously reported. There is, according to Oriani, a considerably loosening of the lattice giving rise to positive deviations from Vegard's Law as shown by Ellwood and Bagley and ¹⁸ by Day. ¹² The loosening of the lattice causes a large vibrational entropy of solution which can account for the large entropy of solution of the alloy. Results obtained by Oriani can be attributed in varying degrees to the other alloys in the system

¹⁹ Geguzin and Pinos reported that from some comparisons of the calculated and experimental equilibrium diagrams that for the gold-nickel system the solidus is 200°C higher than would

be expected from calculation. This finding they attributed to the large difference in atomic radii and the resultant energy of distortion in the lattice.

20

Munster and Sagel in an investigation of the degree of short range order and thermodynamic properties of metallic solutions contradicted the findings of Flinn et al by reporting that the diffuse scattering of X-rays could be attributed to clustering (a preference for like neighbours) in gold-nickel alloys and not to short range order. In support of this contention they forwarded criticisms of some experimental points and the lack of certain mathematical corrections in the previous work. Nagorsen and Averbach studied small angle scattering of X-rays in the gold-nickel system and concluded that scattering occurred through double Bragg reflections. This scattering was purported to be unrelated to any critical scattering due to short range order although they did not concede that short range order is absent from the system but that further work on single crystals would be necessary.

21

The most recent thermodynamic investigation of the system has been by Sellers and Maek whose findings are consistent with previous work. They argue that since the electronic structures of copper and gold are similar and that the 6s band of gold (4s band of copper) will fill the 3d band of nickel, that the magnetic and electronic contributions to

22

the excess entropy of mixing should be similar in both systems.

ΔS^{23} for copper-nickel is negative throughout except at the nickel rich end where it is zero.²³ In the copper-nickel system the vibrational contribution to ΔS^{23} will be small since the size difference between the elemental atoms is small (3%) whereas the large size difference (15%) between gold and nickel will give rise to large dilations of the electronic orbitals^{on} solid solution formation causing a "loosening" of the lattice and a consequent large vibrational contribution to ΔS^{23} .

²²
Sollars and Mack conclude that the quasi-chemical theory and its modified form by Neumann which takes into account the size difference of the atoms, cannot be applied to the gold-nickel system because the theory does not provide for the change in electronic structure of the atoms on solid solution formation, nor does it postulate for systems which do not follow the Kopp-Neumann rule.²⁴

SECTION 3.VACANT LATTICE SITES.

The occurrence of vacant lattice sites in metallic crystals can be attributed to three sources:-

- (1) Vacancies present in all metals in thermodynamic equilibrium with the filled lattice sites.
- (2) Vacancies which arise from electron concentration effects.
- (3) Vacancies which arise in terminal solid solutions due to the effects of overlaps across energy discontinuities in k-space i.e. Brillouin Zone overlaps.

(1) In crystals at temperatures above the absolute zero there is an equilibrium concentration of vacant lattice sites which increases exponentially with temperature. These vacancies arise because of the violent thermal vibrations of the atoms which produce the probability of an atom being ejected from its position to leave a vacant site. The atom may be removed to an interstitial site when the resultant array is termed a Frenkel defect. On the other hand, the Schottky defect results when the ejected atom migrates ^{to} a grain boundary or as ^{is} it most certainly the case to a dislocation. The energy required to form a Frenkel defect is large and consequently the

likelihood of a significant number in a close-packed metallic phase is minimal.

From thermodynamic considerations the presence of vacancies are readily understood.

$$\Delta G = \Delta H - T\Delta S$$

The lattice vacancies once formed, can distribute themselves in many ways within the crystal thus increasing the entropy. However, the enthalpy of the crystal is also increased when vacancies are formed, but provided the $T\Delta S$ term outweighs the enthalpy factor, the free energy of the system is lowered to render the structure more stable.

In simplest terms, taking n as the number of vacancies in a crystal of N atoms then,

$$\frac{n}{N} = \exp. \left(-\frac{\Delta H}{RT} + \frac{\Delta S}{R} \right)$$

25

Huntington and Seitz obtained data for copper which when properly corrected for the entropy term pointed to a value of the order of 10^{-3} (0.1%) for the number of vacancies present near the melting point. More recently Simmons and Balluffi²⁶ obtained a value of 10^{-4} for silver near to the melting point and proposed that 90% of these are present as single lattice vacancies, the remainder as mostly divancies

(2) Vacancies are produced in certain phases to maintain a constant electron concentration thus avoiding energetically

expensive filling of states beyond the peak of the $N(E)$ curve. Early studies based on lattice parameter and density measurements showed that atoms are omitted from the phases of binary and ternary systems based on Ni-Al,^{27,28} Co-Al²⁹ and Fe-Al.³⁰ Böttger and Hume-Rothery³⁵ have given evidence that the γ structure of Cu-Al and Cu-Ga which contains 52 atoms per unit cell is stable up to an electron concentration of 86.5 or 88 but thereafter atoms are omitted from the structure to maintain this value.

(3) Brillouin zone overlaps are claimed by Jones³¹ to cause a contraction of the zone dimensions in k-space in a direction normal to the plane overlapped, which is equivalent to an expansion of the crystal lattice in the same direction in real space.^{32,33} This contention was borne out by Raynor and Hume-Rothery³⁴ and Raynor with respect to the form of the first Brillouin zone of magnesium as elucidated by Jones.³¹ It was shown that sharp changes occur in the variation of the c-spacing at an electron to atom ratio of 2.00/5, whereas the linear variation of the 'a' spacing was maintained because the overlap occurred in a direction which did not affect the 'a' dimensions of the lattice.³⁶ In the Mg-Cd system Hume-Rothery and Raynor reported that changes were detected in both the 'a' and 'c' spacings, corresponding to overlap in two different directions in k-space.

37

38

Studies by Ellwood on the Al-Zn and Al-Mg systems
 //
 and by Ellwood and Bagley on the Au-Ni system revealed
 discontinuities in the variation of lattice parameters with
 compositions and ^{they} were able to correlate these anomalies with
 discrepancies between the theoretical and the measured densities.
 The latter were lower over the range of composition in
 question, pointing to the creation of vacant lattice sites.

39

Lee and Rayner found similar effects in the Sn-In and Sn-Cd
 systems but were able to forward more convincing explanations
 of the phenomena in terms of Brillouin zone overlaps than
 //
 were Ellwood and Bagley. In general terms, the discrepancies
 were attributed to the relative instability created when the
 Brillouin zone continues to be filled after the Fermi surface
 has touched the planes of energy discontinuities. The
 formation of vacancies implies an attempt by the structure to
 maintain a constant electron concentration to render the alloy
 more stable than those which would be present if the high
 energy states were filled. At increasing solute concentration
 the lattice parameter variations again become smooth
 corresponding to the completion of the overlaps.

40

Kudman proposed that the excess vacancies of the
 systems might be explained in terms of a stress relaxation
 in the lattice produced by the creation of vacancies.

He postulated that a solid solution phase consists of a series of contiguous domains of varying degrees of order and that the creation of vacant sites between them would offset the stress effect of each domain relative to its neighbours. This theory, however, did not account for the order of magnitude of vacant sites which had been reported.

As previously stated,⁴² Day was unable to confirm the findings of Ellwood and Bagley for five alloys. Holfrich and Dadd⁴¹ in an investigation of density anomalies in binary aluminium alloys reported similar discrepancies to those of Ellwood but reasoned that an explanation could be found in terms of solidification microshrinkage. This hypothesis was confirmed by preparing an alloy by the vapour diffusion of zinc into aluminium. In this case, the measured and theoretical densities were in agreement. Later, in a general review of this type of excess vacancy concentration,⁴² these same authors concluded that accurate hydrostatic densities of ductile phases having a large freezing range could be obtained only provided the alloys were prepared by vapour diffusion techniques. They agreed that since Sn-In has a narrow freezing range the excess vacancies could not be attributed to shrinkage micro-porosity and that the system probably did contain defect structures. However, further independent work by the⁴³ authors

⁴⁴
and by Ridley showed no significant difference between the
measured and the theoretical densities. Any vacancies
detected were apparently not in excess of that required for
thermal equilibrium.

CHAPTER 2.

ANALYTICAL TECHNIQUESSECTION 1.X-RAY ANALYSIS OF A CRYSTAL LATTICE.

If a beam of monochromatic light falls on a simple two dimensional diffraction grating, the transparent apertures become sources of dispersing wavelets of the same wave length as the incident beam. At some distance from the grating the wavelets combine to form a set of diffracted beams whose spectra are of 1st, 2nd, --- nth order depending on whether the path differences of wavelets emanating from successive apertures are of 1, 2, ---, n wave-lengths. For a grating of interval a , angle of incidence of the beam α_1 , and angle of diffraction α_2 , the path difference is

$$a (\cos \alpha_1 \pm \cos \alpha_2)$$

and for the diffraction angle to be that a spectrum line,

$$a (\cos \alpha_1 \pm \cos \alpha_2) = n\lambda$$

where n is any integer, is a condition which must be satisfied.

In the case of the diffraction of X-rays, a crystal lattice acts in essence as a three dimensional grating. As the beam travels through the crystal, the regularly spaced atoms become the centres of spreading wavelets which form

diffracted beams. If the axes of the lattice are of length a , b and c , the respective angle of incidence $\alpha_1, \beta_1, \gamma_1$, and the angle between the diffracted beams and the axes $\alpha_2, \beta_2, \gamma_2$, the conditions for diffraction are given by three *Laue* equations.

$$a (\cos \alpha_1 \pm \cos \alpha_2) = h \lambda$$

$$b (\cos \beta_1 \pm \cos \beta_2) = k \lambda$$

$$c (\cos \gamma_1 \pm \cos \gamma_2) = l \lambda$$

where h , k and l are integers which correspond to n for a two-dimensional grating. It is clear that a diffraction spectrum for a three dimensional grating will be infrequent since three equations must be satisfied simultaneously.

THE BRAGG LAW.

The diffraction of X-rays by a three dimensional lattice governed by the above conditions can, as shown by W.L. Bragg, be regarded as a reflection of X-rays by the lattice planes. Bragg's Law states that if a diffracted beam is produced by X-rays passing through a crystal, it must be in such a direction that it may be considered as derived by a reflection of the incident beam from one of the sets of lattice planes. This occurrence is governed by the equation

$$n \lambda = 2d \sin \theta$$

θ = glancing angle of incidence

d = spacing between the successive lattice planes
in the set of lattice planes.

n is an integer.

THE CELL EDGE.

The cell edge " a " for the cubic system is related to the interplanar distance d in terms of Miller indices h' k' l' which define a set of crystallographic planes, by the equation.

$$a = d \left((h')^2 + (k')^2 + (l')^2 \right)^{1/2}$$

Hence, the Bragg condition may be written as

$$a = \frac{\lambda}{2} \frac{\left((h'n)^2 + (k'n)^2 + (l'n)^2 \right)^{1/2}}{\sin \theta}$$

In terms of *Lane* indices since $h = nh'$, $k = nk'$, $l = nl'$,

$$a = \frac{\lambda}{2} \frac{\left(h^2 + k^2 + l^2 \right)^{1/2}}{\sin \theta} = \frac{\lambda}{2} \frac{\sum h^2}{\sin \theta}$$

THE DEBYE-SCHERRER POWDER METHOD.

The powder method is an ideal means for the study of crystalline solids which exist in a fine state of sub-division or as an agglomerate mass of minute crystals. Obviously, it is, therefore, well suited to the investigation of metallic phases.

When a narrow collimated beam of X-rays falls upon a specimen of the powder under scrutiny, some of the crystal fragments will, since their orientations are perfectly random, be positioned in such a direction as to satisfy the Bragg condition for reflection. The diffracted beams with the same indices h, k, l all lie upon the surface of a cone of semi-vertical angle 2θ . To record the entire spectrum the photographic film is formed into a cylinder concentric with the specimen thus allowing low order and high order ($\theta \rightarrow 90^\circ$) reflections to be detected. A complete pattern of lines is thus obtained, each line corresponding to a segment of a particular diffraction *halo*.

For a cubic crystal the lines may be readily indexed since,

$$a^2 = \frac{\lambda}{2} \cdot \frac{\sum h^2}{\sin^2 \theta}$$

Hence, the only task is to determine the values of the integers $\sum h^2$ such that

$$\frac{\sum h^2}{\sin^2 \theta} = \text{a constant.}$$

For crystals of progressively lower symmetry the photographs become more complex and indexing is correspondingly more difficult.

DAUBE-SCHERRER CAMERAS.

The most commonly used Debye-Scherrer cameras are 9 cm. and 19 cm. diameter, the larger the camera the longer the exposure time required, but the greater the resolution. Therefore, in the study of simple cubic structures, the smaller camera is satisfactory. Figs. 3 and 4 are of the 9 cm. camera used in ^{the} present investigation. The specimen is fitted centrally and rotates without any lateral movement. On the periphery of the camera are two knife edges which press tightly against the film when it is wound round the camera. The film is held by a strip of spring steel. The camera cover houses a motor drive which rotates the specimen. Should the specimen not be rotated the diffraction lines are spotty because only a limited number of crystal fragments located at the required Bragg angle are presented to the incident beam.

The camera is designed for a Van Arkel arrangement of the film. This arrangement makes the maximum use of the high order reflections since these give the most accurate measurements of the lattice parameters. The collimated beam of X-rays enters through a hole punched in the film and any undiffracted rays are absorbed by a glass plate containing a suspension of lead oxide. Because the high angle lines

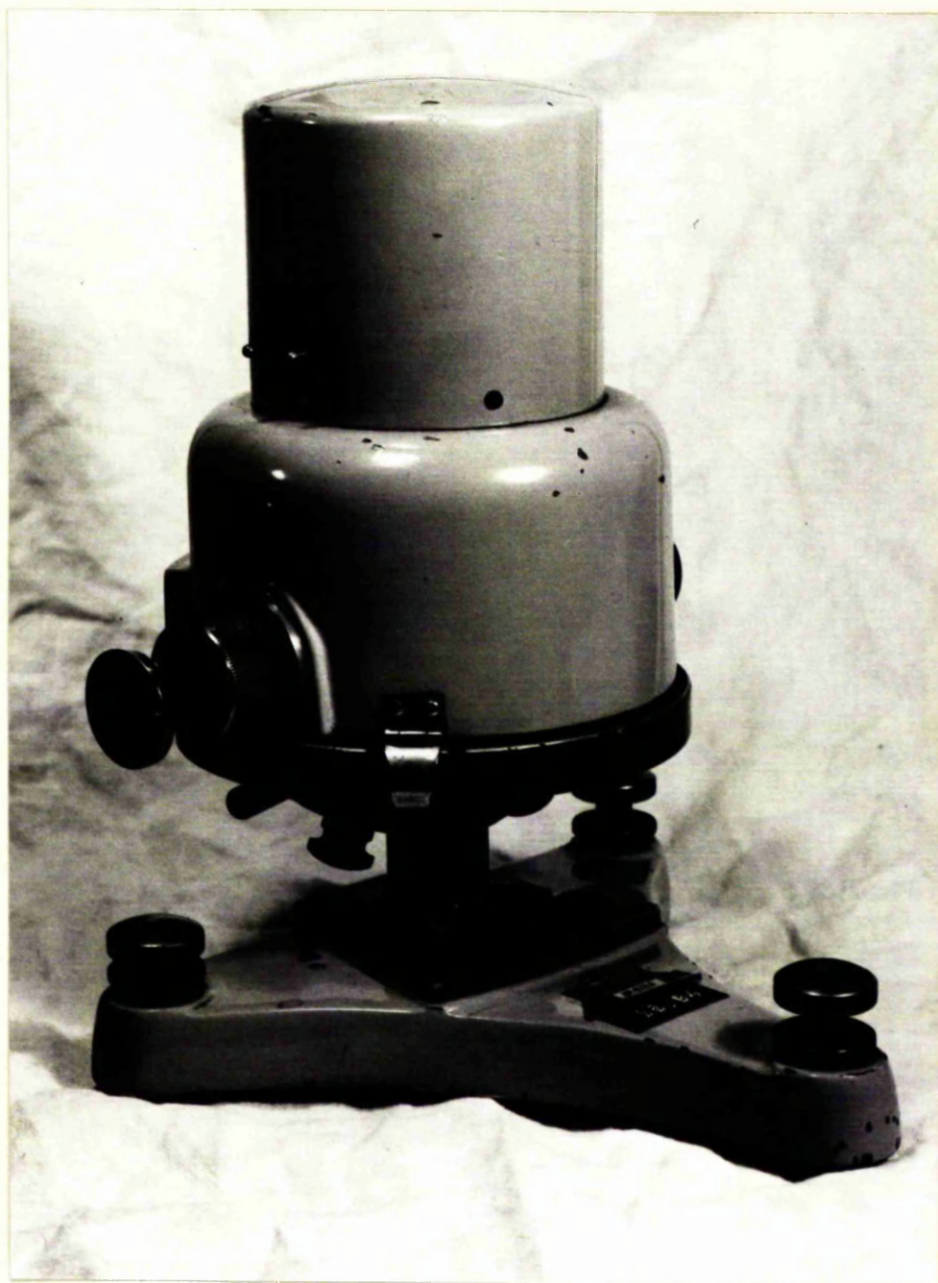


FIG. 3.

DEBYE-SCHERRER X-RAY CAMERA

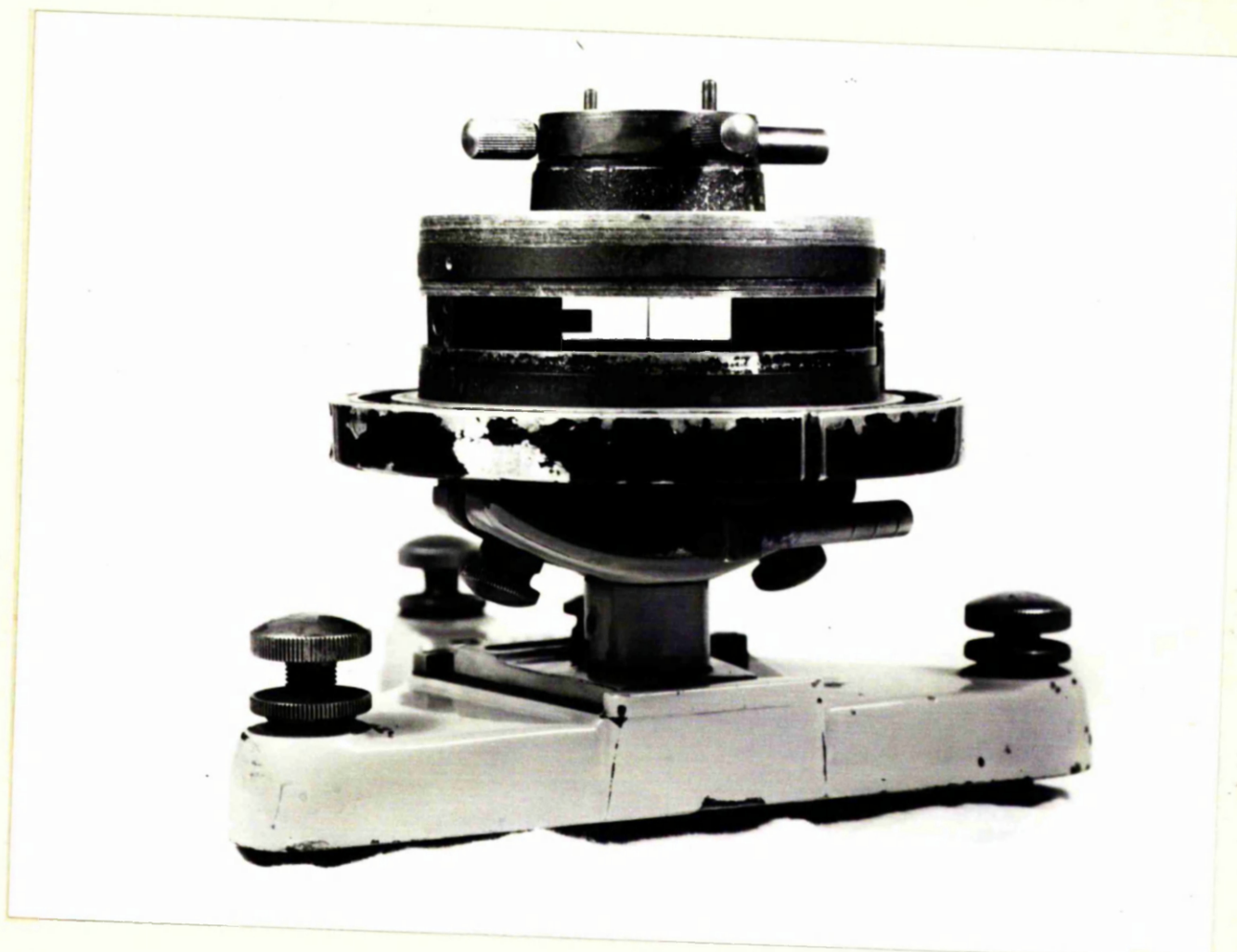


FIG. 4.

DREYER-SCHERRER X-RAY CAMERA

are positioned on either side of the punched hole, the effects of film shrinkage caused during developing, are minimised as far as the high angle lines are concerned, on account of the short distance of separation.

MEASUREMENT OF θ

The measurement of the angle θ_c which corresponds to the whole exposed length of the film is determined from the camera diameter and the distance between the knife edges, both of which can be measured by vernier calipers. θ_c is a constant for any particular camera. By a proportionality, the angle corresponding to the distance between two equivalent lines can be calculated.

THE MEASUREMENT OF THE FILM.

The distance between the equivalent lines and between the knife edges are measured on a film comparator ^{is} on which there was a metric scale and an accurate vernier scale fitted with a hairline. Since the instrument is of a high quality, accurate readings were obtained to within the limits of the instrument, i.e. down to 0.025 m.m.

ELIMINATION OF SYSTEMATIC ERRORS FROM THE LATTICE PARAMETER DETERMINATIONS.

In the determination of lattice spacings there are six sources of error which may give rise to inaccurate values.

1. The finite length of the specimen irradiated by the beam.
2. Film shrinkage.
3. Refractive index of the crystallites for X-rays.
4. Eccentricity of the specimen.
5. Distribution of X-ray intensity in the focal spot.
6. Absorption of X-rays in the specimen.

It has been shown that the error due to (1)
⁴⁵⁴⁶
 is negligibly small.

The effects of (2) are eliminated by comparing the calculated distance between the knife edges and the distance measured on the developed X-ray film. For refractive index, correction is very slight, ⁴⁷⁴⁸ ranging from 1 part in 10,000 to 1 part in 200,000 and for the present purposes it may be omitted. It has been found that any errors due (4), (5) and (6) are most easily eliminated by extrapolation methods since the errors become minimal at

$\theta = 90^\circ$ i.e. extreme back reflection along the path of the incident beam. A graph of 'a' against almost any function of the Bragg angle θ would be satisfactory but for ease of determination it is preferable to choose one which is as linear as possible over the entire angular range.

⁴⁹
 It has been shown that if the focal point is

taken as an idealised point source of radiation from which the beam has diverged that the error in lattice parameter is proportional to $\cos^2 \theta / \sin \theta$. In a well constructed camera, the specimen can be positioned sufficiently close to the axis of rotation to render any eccentricity error negligible. Nelson and Riley⁵⁰ showed experimentally that the only function of θ which gives a linear plot over the entire angular range is

$$f(\theta) = \frac{1}{2} \left(\frac{\cos^2 \theta}{\sin \theta} + \frac{\cos^2 \theta}{\theta} \right)$$

To obtain the correct value of the lattice parameter, the apparent 'a' values are plotted against $f(\theta)$ and the graph extrapolated back to $\theta = 90^\circ$ ($f(\theta) = 0$).



FIG. 5.

CUPPELL AND LEAD FOIL.

ANALYSIS OF GOLD.

CUPELLATION

The gold content of an alloy of composition sufficiently great for macroanalysis may be satisfactorily determined by cupellation which makes use of the immiscibility in the liquid state of gold and lead. 200 m.g. of powdered alloy, in the present case gold-nickel, are wrapped in high purity lead foil and placed in the basin of a cupell (fig. 5) which is then transferred to a muffle furnace at 900°C . The lead once molten takes nickel but not gold into solution. A cupell is made of a refractory material, its function being to absorb the lead phase. Gold atoms in the melt agglomerate and after the lead has disappeared a bead of gold remains in the basin of the cupell. The gold can then be weighed to determine the composition of the alloy.

When this operation is performed carefully, a high degree of accuracy is obtainable. It is necessary that a sufficient quantity of lead foil is used to ensure complete solution of nickel.

CHAPTER 3

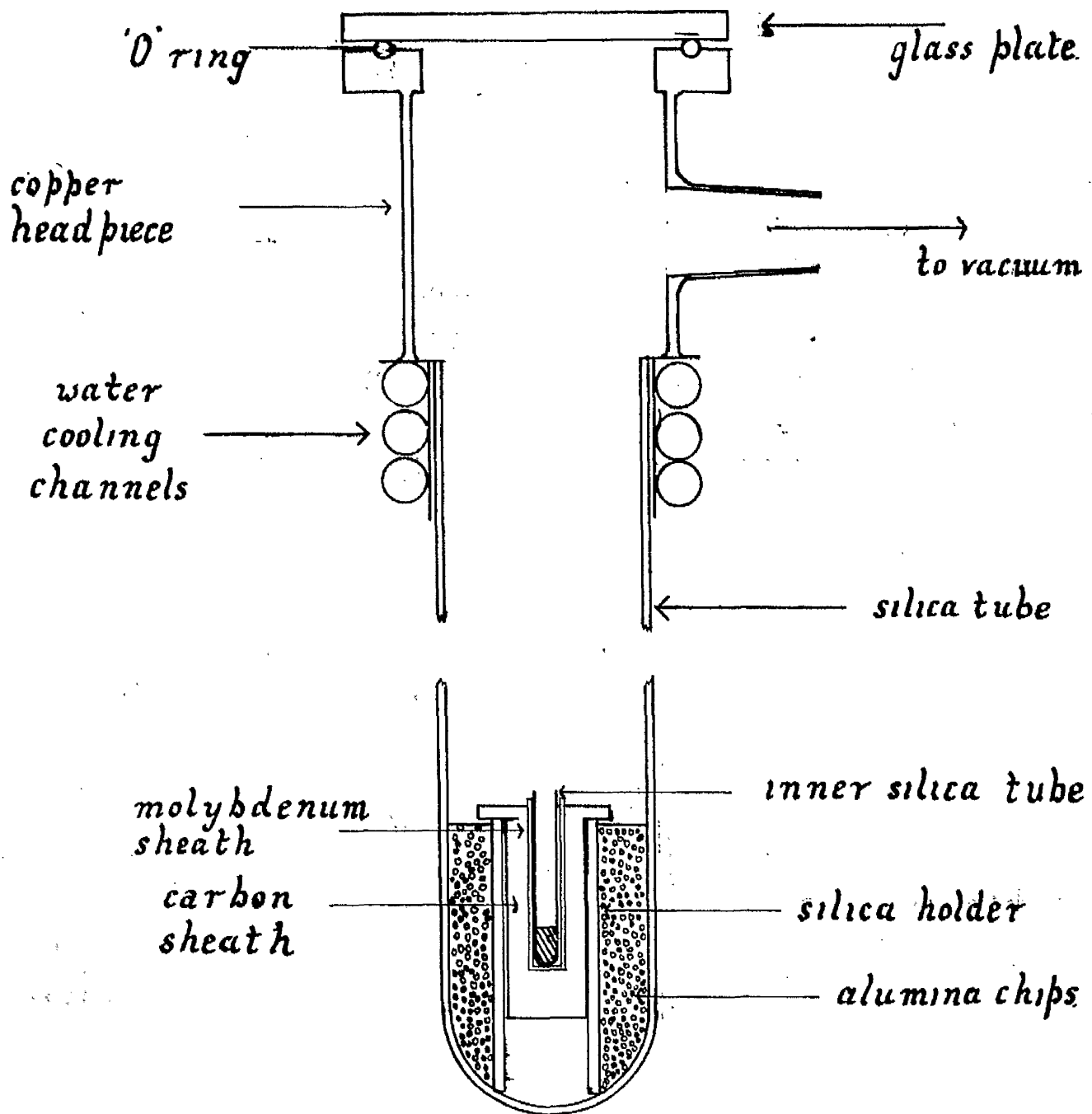


Fig. 6. Apparatus for melting alloys-1.

EXPERIMENTAL PROCEDURE.SECTION 1.PREPARATION AND ANALYSIS OF GOLD-NICKEL ALLOYS-1

Gold of 99.99% purity and nickel of 99.999% purity both obtained from Johnson Matthey Ltd. were used to prepare 4 gm. samples of these alloys:-

<u>Atomic % Ni.</u>	<u>Pt. % Ni.</u>	<u>Melting Point °C</u>
0	0	1063
5	1.54	1045
10	3.20	1030
15	4.99	1015
20	6.93	1000
25	9.02	980
30	11.32	960
35	13.82	954
40	16.56	950
45	19.58	960
50	22.94	980
55	26.68	1010
60	30.86	1050
65	35.66	1085
70	40.98	1130
75	47.18	1160
80	54.35	1240
85	62.77	1290
90	72.80	1330
95	85.0	1400
100	100	1453

The component metals were melted under vacuum to form alloys in the apparatus shown in fig.6. In principle, the apparatus is the same as that used by Bagley⁵² but in the course of experimentation certain modifications had to be made.

The gold and nickel were held in a small silica tube of 7 mm. diameter which had been previously cleaned in either chromic acid or aqua regia to remove any material which might have caused contamination of the alloys. A thin molybdenum sheath into which the silica tube was lowered separated the silica from the graphite rod since contact between these substances was later shown to be deleterious to obtaining a good vacuum system. The graphite rod was held centrally by a length of silica tubing which was surrounded by a packing of fused alumina. This assemblage so far described was contained in the lowest 6 inches of a 2 inch diameter, 24 inches long thick walled round bottomed silica tube. The large outer silica tube was held by "Apicon W" wax inside a copper attachment on which was an outlet to vacuum and on top was a thick glass plate resting on a rubber O-ring. To prevent melting of the wax through heat transmitted up the tube, water channels were built in to the apparatus to cool the wax.

The heating of the metals was effected by a high frequency induction coil. Since the load of metal to be melted was so small, the heat transference had to be aided by conduction through the graphite rod. Under the circumstances heating was essentially by conduction although some transfer of energy by high frequency induction provided a stirring of the melt.

Before heating commenced, the entire chamber was evacuated down to 10^{-5} mm. Hg by an oil diffusion pump backed by a rotary pump. The pressure reading was taken from an all glass vacuostat. When the metals reached a temperature of 900°C recorded by a disappearing filament radiation pyrometer, that temperature was maintained to allow outgassing of the graphite and fused alumina packing. The metals were then heated to 150°C above the melting point of the alloy to ensure homogeneity of the melt and exclusion of any occluded gases. After solidification, the alloy was remelted for further outgassing, and then cooled down to room temperature. Satisfactory ingots, free from surface blemishes and oxidation were obtained.

The diagram of fig. 6 was the final melting apparatus. Initially, the lower assemblage was that used by Bagley which differed from that shown in the following respects:-

- (a) There was no molybdenum sheath to prevent physical contact between the inner metal containing silica tube and the graphite rod.
- (b) The graphite rod was of a small diameter and was ^{not} held _{in} silica ^{but} and ^{not} alumina.

(c) A packing of graphite powder was used to cut down radiation losses.

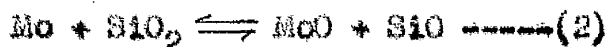
Pure nickel was melted first of all since the highest temperature of all the melts, 1600°C , was required, thus fully testing the apparatus. At about 1400°C the vacuum was lost and blue grey discharge was produced when the system was tested by a tesla coil. The gas being formed was suspected to be carbon monoxide from the reaction



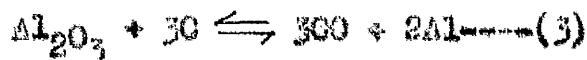
Moreover, the small silica tube became whitened by what was perhaps reformed SiO_2 . Vapour pressure data^{5/} revealed these values:-

<u>Temp $^{\circ}\text{C}$</u>	<u>pCO in reaction (1) (mm.Hg)</u>
1027	8.46×10^{-2}
1400	50.3

Hence, reaction (1) was thermodynamically possible. In order to counteract this effect the silica was surrounded by molybdenum whose vapour pressure data did not show any tendency toward the reaction.



The melting of pure nickel was repeated but at 1500°C the vacuum was again lost due to the reaction:



<u>Temp °C</u>	<u>n CO in reaction (3) (mm.Hg)</u>
1400	2.4×10^{-1}
1500	1.32

Alumina was discarded from the system except for the packing, in which region the temperature was not sufficiently high for any reaction to take place.

Graphite powder was eliminated because it required, for outgassing, unsuitably long periods of evacuation at high temperatures. Moreover its value in preventing radiation losses was not appreciated since the melting of all the alloys could be achieved when fused alumina was used as a packing material.

All of the alloys were reweighed after melting. The losses in weight, compared with the made up compositions, never exceeded 0.07 at.%,

ANNEALING.

The ingots in batches of six or seven were sealed off under vacuum in transparent silica tubes in the same manner as did Bagley.⁵² To prevent interdiffusion, the ingots were separated from each other by small pieces of silica. An anneal was carried out at $900^{\circ}\text{C} \pm 10^{\circ}\text{C}$ for four weeks to ensure homogeneity of the solid solution phases. When the annealing time had been completed the tubes were withdrawn from the furnace, the ends broken and the alloys immediately

quenched into cold water to retain the solid solution.

Lattice parameters were determined on these ingots but, as explained in Chapter 4, the values were shown to be in error. This error arose from the manner in which the alloys were annealed.

SECTION 2.PREPARATION AND ANNEALING OF GOLD-NICKEL ALLOYS -2

A series of alloys of the same compositions as previously, were melted in evacuated (10^{-5} mm.Hg) silica tubes. In this manner the entire range of alloys could be melted more quickly than in section 1. Heating was effected by a small closely wound induction coil enhanced by conduction through a graphite block as shown in fig.7. When the alloys were molten the high frequency induction current was switched off and the melt shaken manually to ensure homogenisation. The losses on melting were again less than 0.1wt.%. Some surface blowholes were present on the alloys but there was no evidence of oxidation.

ANNEALING.

The ingots were annealed at $900^{\circ}\text{C} \pm 100$ for two weeks in separate evacuated silica tubes and quenched into water after annealing.

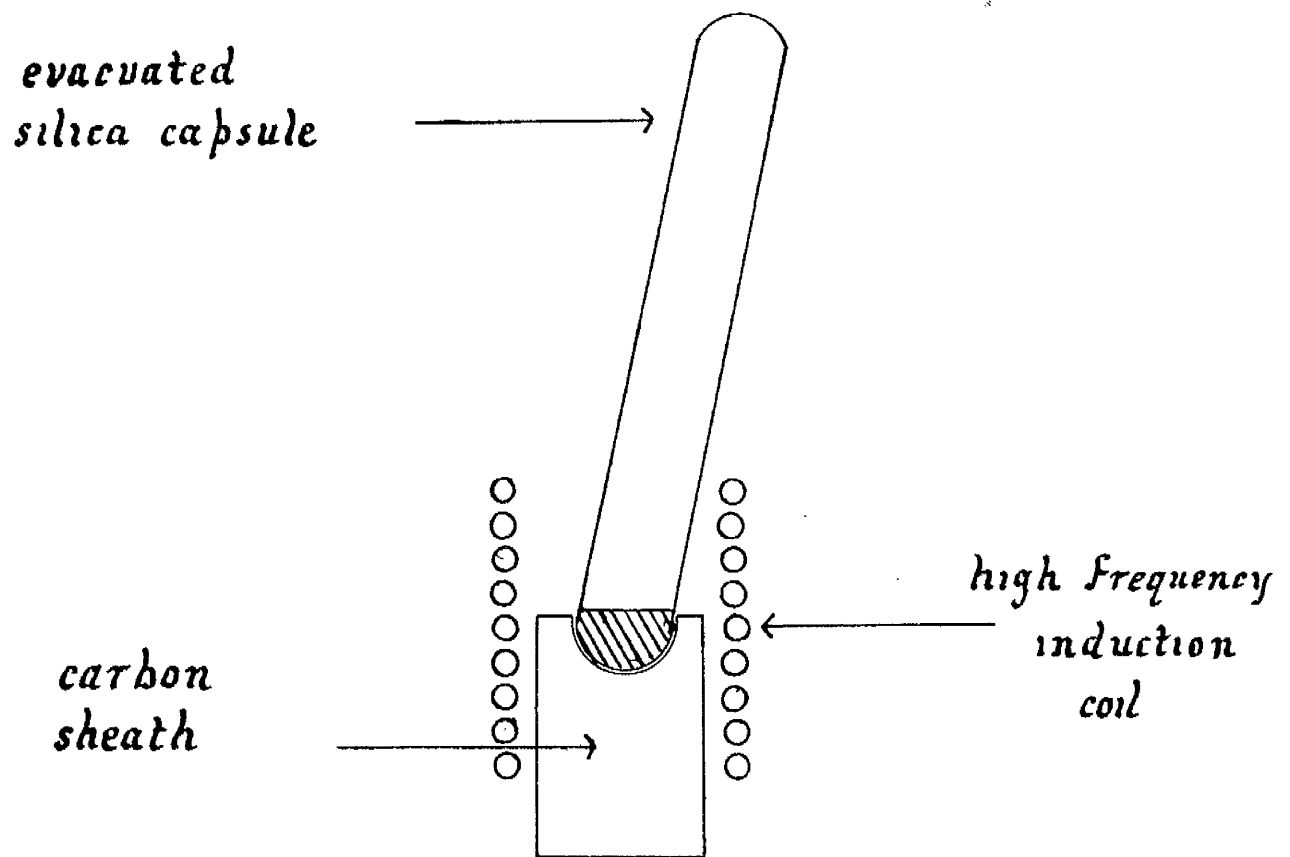


Fig. 7. Apparatus for melting alloys-2

SECTION 3.PREPARATION AND HEAT TREATMENT OF X-RAY POWDER SPECIMENS.

The powder samples were obtained by filing the ingots with a precision Swiss file of No.4 cut. Since the filings had to be stress-relieved which effectively meant annealing for one hour in the solution range at 900°C , the powders were introduced to small silica quills 0.5mm diameter and 0.2 mm wall thickness. For each alloy three specimens were prepared, the filings coming from different parts of the ingot. In this way the homogeneity of each ingot could be ascertained. Some quills were sealed off under vacuum but there was no noticeable effect on the powder photographs or lattice parameters compared with samples sealed in air. In the latter case, there was no evidence of oxidation after annealing because the volume of air present was so small.

The quills were placed in a mild steel container at $900^{\circ}\text{C} \pm 1^{\circ}\text{C}$. A length of heat resistant wire was attached to the container so that after annealing the container could be withdrawn rapidly from the furnace and plunged into cold water.

SECTION 4.DETERMINATION OF LATTICE PARAMETERS.

The lattice parameters of gold-nickel alloys were determined by the powder method in a 9 cm. Debye-Scherrer camera with a Van Arkel arrangement of the film. Past users of the camera had determined the camera constant. The distances, however, between the knife edges and the camera diameter, were re-checked using accurate measuring instruments. The camera constant then calculated was in agreement with the previously determined value.

The most suitable single source of radiation for this series of alloys is that from a copper target. Lattice spacings were determined from the diffraction lines produced by copper $K\alpha_1$ radiation. The $K\alpha_2$ lines were ignored and the $K\beta$ radiation was absorbed by a nickel filter.

Distances between the lines were measured to ± 0.012 mm. by being placed against a scale on which was a Cursor and accompanying Vernier scale. The apparent 'a' values were plotted against $f(\theta)$ according to the method of Nelson and Riley⁵⁰. All values of lattice parameter were determined in Kx units ($\lambda = 1.00202$ Kx)⁵³. In a few cases poor diffraction lines were obtained because of inhomogeneity of the ingots which were then remelted and re-annealed since

experience showed that re-annealing alone could not give homogeneity because of slow diffusion in the solid state.

Lattice parameters were adjusted to 25°C in the manner described by Ellwood and Bagley. Nickel and Gold have coefficients of linear expansion of $14.4 \times 10^{-6} \text{ }^{\circ}\text{C}^{-1}$ and $13.00 \times 10^{-6} \text{ }^{\circ}\text{C}^{-1}$ respectively and the coefficients for intermediate compositions were taken from a linear plot of these values.

SECTION 5.DETERMINATION OF DENSITIES.

The densities of the alloys were determined by the use of a density bottle. A density bottle has a volume V_1 determined from the weight of fluid required to fill it and the density of that fluid. If a specimen is placed in the bottle, the new weight and hence volume V_2 of fluid required to fill the bottle can be calculated. The volume of the specimen $V = (V_1 - V_2)$ is then obtained.

The fluid used in the present work was benzyl alcohol⁵⁴ which has excellent wetting properties superior to water. It has a stable density whose variation with temperature has been well established.⁵⁵

Evidently, the error in the volume of the bottle $\pm \delta V$ is also the error in the volume of the specimen since the introduction of a proportionality error for the latter is unjustifiable. Hence, the feasibility of the method hinges on a density bottle of a volume as close as possible to ^{the} order of the specimen volume and whose volume could be determined to within very precise limits.

CONSTRUCTION OF A DENSITY BOTTLE.

A density bottle shown in fig. 8 was made from a standard "quickfit" B.14 cone and socket. The lower part was



FIG. 8.

DENSITY BOTTLE.

prepared by the ordinary glass blowing technique of inducing a flat bottom in a cylinder of pyrex glass. To manufacture the stopper, the ground glass section was formed into an approximate hemisphere, after which the capillary tube was positioned centrally against the hemisphere and fused to it. The area of glass covering the capillary column was then heated to fluidity and blown out. A section of clear glass above the ground cone was then heated until it collapsed onto the central tube. Heating was continued until the capillary had been reduced to about one-third of its original diameter. After being annealed the glass was cut at this point by a diamond wheel.

After manufacture, cracks appeared in the stopper because of the differential cooling rates of thick glass of the capillary tube and the thin glass of the outer tube. It was experienced that even after very careful annealing under a progressively cooler flame, that cracks still appeared very soon after removal from the flame. To overcome this problem, the entire workpiece after flame annealing was immediately transferred to a furnace at 560°C at which temperature pyrex glass is slightly plastic. The stopper was then cooled in the furnace down to 300°C where stresses due to differential cooling rates ceased to be operative. No cracks appeared and this one bottle was used to determine the densities of all the alloys.

VOLUME OF THE DENSITY BOTTLE.

The density bottle was cleaned, dried and weighed repeatedly until a constant weight ($\pm 0.0001\text{g}$) was obtained. An arrangement shown in fig.9 was constructed to allow benzyl alcohol to be introduced under vacuum. Benzyl alcohol was drawn from a reservoir through a tube of P.T.F.E., control being effected by a screw clip. The system was evacuated by mercury diffusion and rotary pumps and closed off at A. Benzyl alcohol was then drawn up as far as the screw clip. After further evacuation, the system was again closed at A and benzyl alcohol drawn in to fill the bottle. Evacuation was continued to remove the volatile impurities and air which evolved vigorously from the fluid. When no more bubbles of gas appeared on tapping, the system was closed off at A and air allowed to enter the chamber through B. Some fluid had spilt over into the chamber because of the violent outgassing. This volume was collected in a clean syringe and introduced to the bottle. The bottle was then allowed to stand for 30 minutes to allow the fluid to come to equilibrium with room temperature, after which the temperature was read ($\pm 0.05^\circ\text{C}$) by a mercury thermometer.

The stopper was inserted and turned tightly into the socket. During this operation any excess fluid was forced up through the capillary. The top of the stopper was

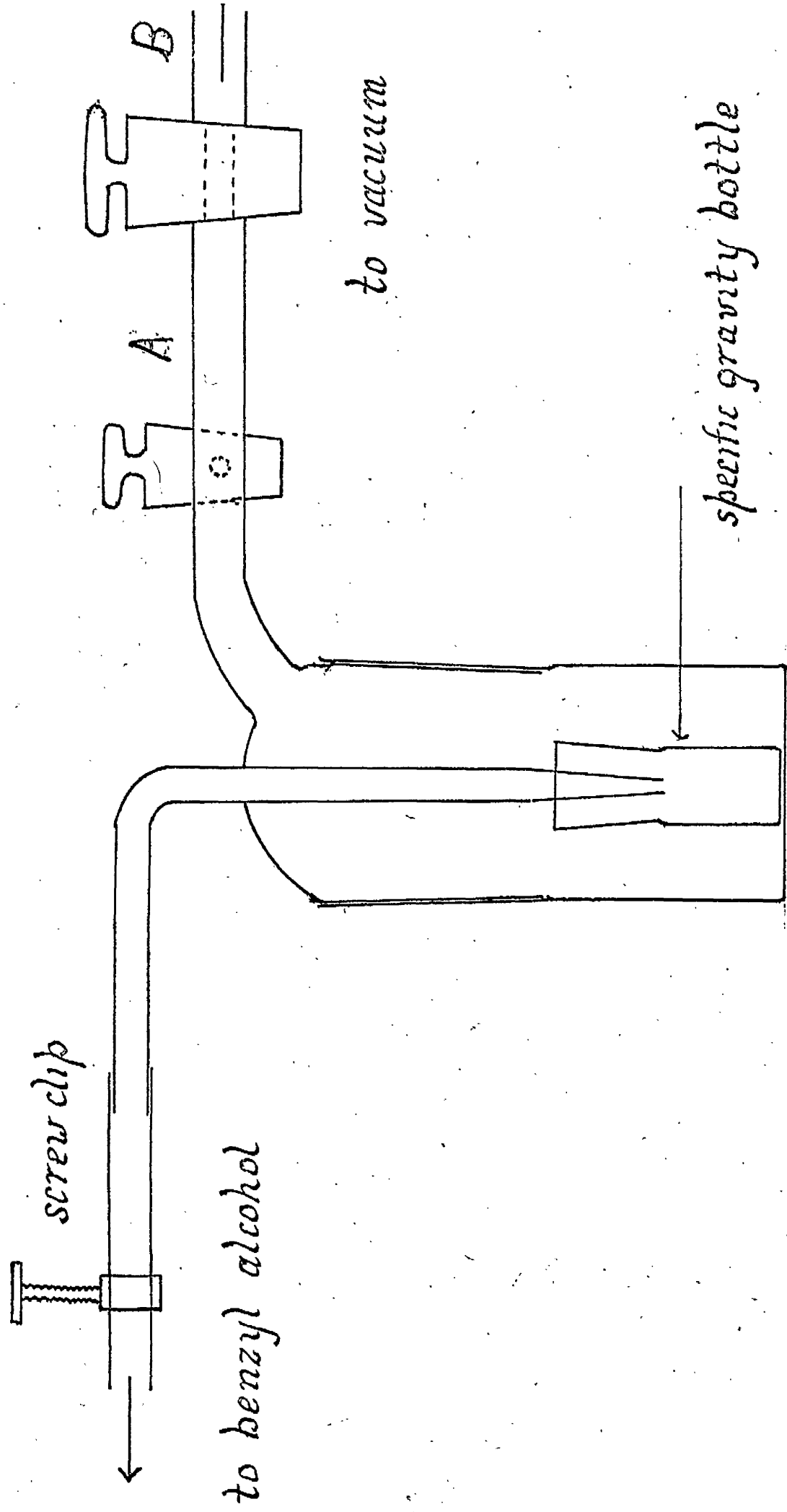


Fig 9 . Density Apparatus

carefully wiped with absorbent paper taking care to note that no benzyl alcohol was removed from the capillary, a fact ensured by the very small diameter of the top of the capillary.

To remove any excess benzyl alcohol the cylindrical surfaces were carefully rinsed with benzene and acetone. The bottle was then weighed.

The temperature variation of the density of benzyl alcohol is given by the formula:⁵⁵

$$\rho_t = \rho_0 + 10^{-3} A (t-t_0) + 10^{-6} B (t-t_0)^2, \quad t_0 = 0^\circ\text{C}$$

$$\rho_0 = 1.0609 \quad A = -0.7683 \quad B = -0.4590$$

The volume of the bottle was determined five times to give a mean volume of $3.0376 \text{ ml.}^3 \pm 0.0002 \text{ ml.}^3$. To verify the formula, the above procedure was repeated but with some high purity mercury in the bottle. Some time was allowed for any occluded air to be removed from the mercury prior to the introduction of benzyl alcohol.

The density of mercury at 0°C has been determined⁵⁶ by Batencas and Alonso, and the variation of density with temperature by Harlow⁵⁷ and by Beattie et al.⁵⁸ When the summation was made of the volume of mercury and the volume of benzyl alcohol above it, the result was $3.0376 \text{ ml.}^3 \pm 0.0002 \text{ ml.}^3$

Hence, the feasibility of the method was established.

DENSITIES OF GOLD-NICKEL ALLOYS.

An alloy was positioned in the density bottle and the vacuum system evacuated for 30 minutes to remove any air from the alloy surface. Benzyl alcohol was allowed to enter, evacuation being continued until no bubbles appeared on tapping. The volume and hence density of the specimen was determined.

The measured density D_M was compared to the theoretical density D_{TH} calculated from the formula:

$$D_{TH} = \frac{mMN}{a^3}$$

m = mass of unit atomic number = 1.6603×10^{-24} g.
 M = composite atomic weight
 N = Number of atoms per unit cell (4 for the cubic system).
 a = Lattice parameter in centimetres at 25°C

The measured densities were adjusted to 25°C by correcting the volume to that temperature by the formula:

$$V_{25} = V_t (1 + 3\alpha(25 - t))$$

V_{25} = volume at 25°C
 V_t = volume at $t^\circ\text{C}$
 α = coefficient of linear expansion.

Six of the alloys (5, 10, 15, 20 and 45 at.%Ni.) showed measured densities which were considerably less than their theoretical densities. Since shrinkage porosity was the suspected cause, the centres of these alloys were drilled out and the density determination were repeated. The values for four of the alloys then agreed with their theoretical

densities.

In the other two cases, 10 and 45 at.-% Ni, agreement was not reached. The alloys were then filed to a powder whose density was then measured. This method of density determination easily lends itself to studies of powder volumes. Theoretical and measured densities now agreed, pointing to some form of microporosity in the original ingots.

CHAPTER 4c

SECTION 1.LATTICE PARAMETERS OF GOLD-NICKEL ALLOYS.

Lattice parameters of gold-nickel alloys prepared and annealed by the first techniques were not in agreement with previous work. In addition the lattice parameters of pure gold and pure nickel did not agree with established values.⁵⁹ The determined values were 4.0652 Kx and 3.5221 Kx for gold and nickel respectively as opposed to the previously reported values of 4.0703 Kx and 3.5168 Kx.

In order to test the X-ray technique lattice parameters were determined of the as received gold and nickel, giving the values of 4.0702 Kx and 3.5168 Kx. The gold and nickel ingots as prepared were reduced on a turning lathe and filings from powder specimens taken from the reduced section. The measurements of 'a' spacing agreed with the as received gold and nickel. It appeared, therefore, that some form of surface pickup had taken place, probably during the annealing stage.

The lattice parameter of the prepared gold was lower than would have been expected, a possible explanation being the pickup of nickel at the surface. Since the

alloys were separated from each other during the annealing time, the possibility of diffusion in the solid state between the alloys was eliminated. The other manner of mass transference was by deposition from the vapour phase. An indication of likelihood of such a process was clarified by applying Langmuir's equation for adsorption onto a surface.
60
For a vapour in equilibrium with a solid the rate, m , at which molecules of the vapour phase strike the surface of the solid is given by:

$$m = \left(\frac{M}{2\pi RT} \right)^{\frac{1}{2}} p$$

M = molecular weight of substance
 R = gas constant = 8.31×10^7 ergs.
 p = vapour pressure of adsorbant in dynes/cm²
 m is given in g/cm²/sec.

For the adsorption of gold from the vapour state onto gold at 900°C.

$$\begin{aligned} \text{Vapour pressure of gold} &= 2.37 \times 10^{-4} \text{ dynes/cm}^2 \\ m &= 4.25 \times 10^{-9} \text{ g/cm}^2/\text{sec.} \end{aligned}$$

Therefore, after four weeks the weight W_{Au} of the total number of atoms which would have struck the surface is 1.028×10^{-2} g.

The corresponding calculation for nickel gives:

$$\begin{aligned} \text{Vapour pressure of nickel} &= 7.77 \times 10^{-6} \text{ dynes/cm}^2 \\ m &= 7.5 \times 10^{-11} \text{ g./cm}^2/\text{sec.} \end{aligned}$$

After four weeks $W_{Ni} = 1.8 \times 10^{-4}$ g.

These values of W_{Au} and W_{Ni} are calculated from equilibrium considerations whereas in the present problem solid gold was present as a sink for nickel atoms arriving from the vapour phase and vice-versa for solid nickel. In general terms, had the annealing time tended towards infinity all of the alloys in the same capsule would have picked up gold and nickel atoms in sufficient quantity to equalise their compositions and then exist in equilibrium with each other. Under the conditions of the annealing procedure equilibrium did not exist and therefore concentration changes were taking place.

Langmuir's equation gave an indication that the weight transference of metals was very small, but very small quantities in only the surface layers from which the powder specimens were taken are sufficient to cause detectable errors in the lattice parameter measurements. The erroneous 'a' values for gold and nickel correspond to composition changes of 1 at.%,

To confirm this hypothesis, 40 mg. of powder were taken from the surface of the as melted nickel and analysed for gold by cupellation. A minute quantity of gold was found to be present, confirming the proposed explanation of the erroneous results.

SECTION 2.LATTICE PARAMETERS OF GOLD-NICKEL ALLOYS - 2

The lattice parameters of alloys in the gold-nickel system are shown in table I together with the values obtained by other investigators. A high measure of agreement is evident. The present results are very close to those of ¹²Day except at 90 at.% nickel. Composition errors by one of the workers would account for this fact. The values of ¹⁰Kubaschewski and Ebert were read from a poor quality graph in their paper. Therefore, the figures shown may not be very accurate.

The graph of lattice parameter against composition (fig. 10) shows a smooth curve more complete than that of Day and with no anomalous variations over certain compositions as reported by Ellwood and Bagley. At 40 and 55 atomic per cent nickel the points appear to be slightly above the curve. This observation is confirmed in fig. 11 which shows the deviations of the alloys from Vegard's Law which in these alloys are large and positive.

TABLE I

Lattice parameters of Gold-Nickel Alloys at 25°C (Kx units)

Atomic % Ni	Present	Day	Kubaschowski and Ebert
0	4.0702	4.0702	4.0700
5	4.0497		4.0566
10	4.0280	4.0271	4.0280
15	4.0080		4.0052
20	3.9834		
25	3.9600		
30	3.9347	3.9352	
35	3.9105		
40	3.8897		
45	3.8593		
50	3.8334	3.8325	
55	3.8093		
60	3.7771		
65	3.7511		
70	3.7215	3.7216	
75	3.6915		
80	3.6580		
85	3.6287		
90	3.5908	3.5863	
95	3.5559		
100	3.5168	3.5168	

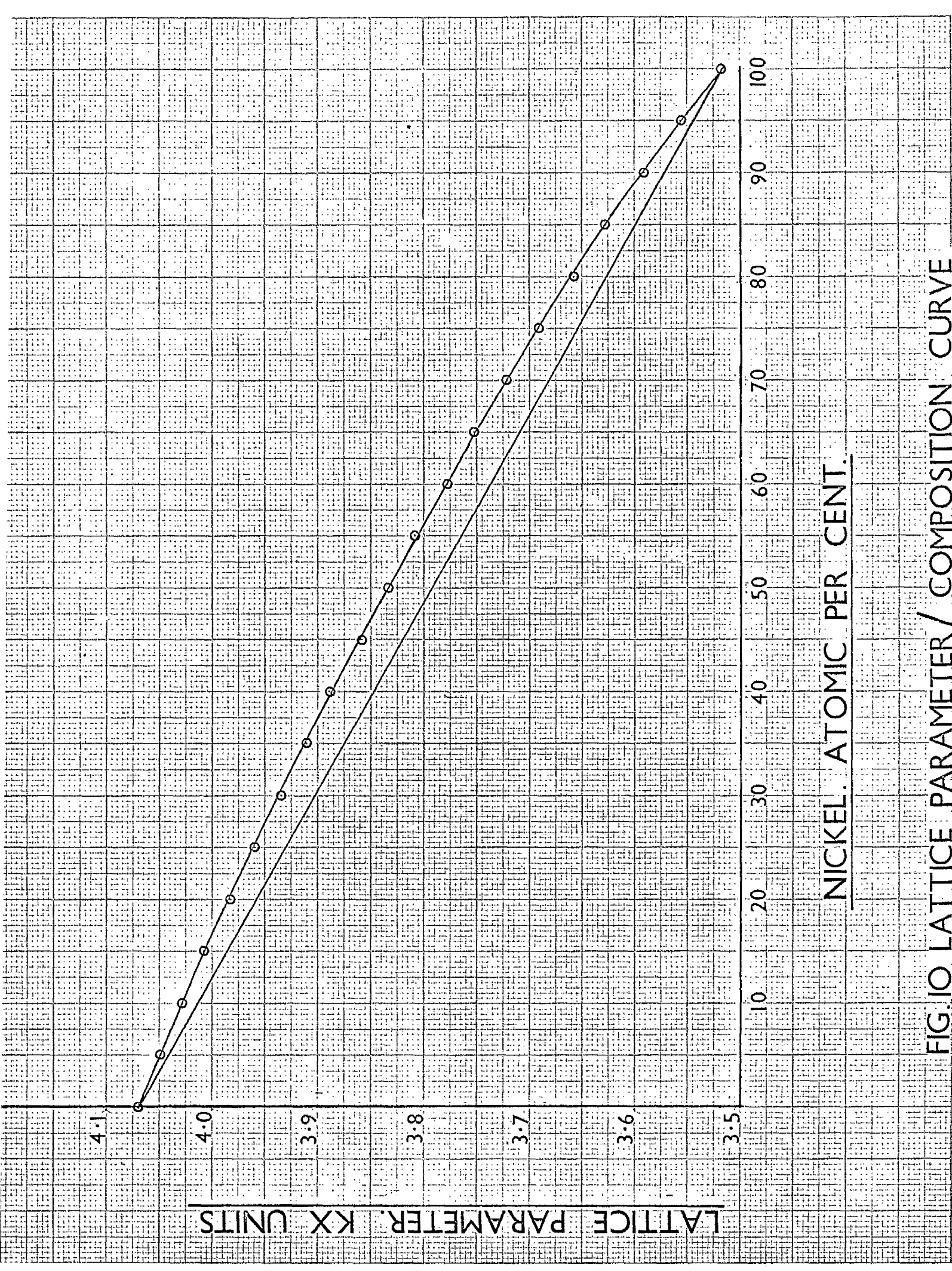
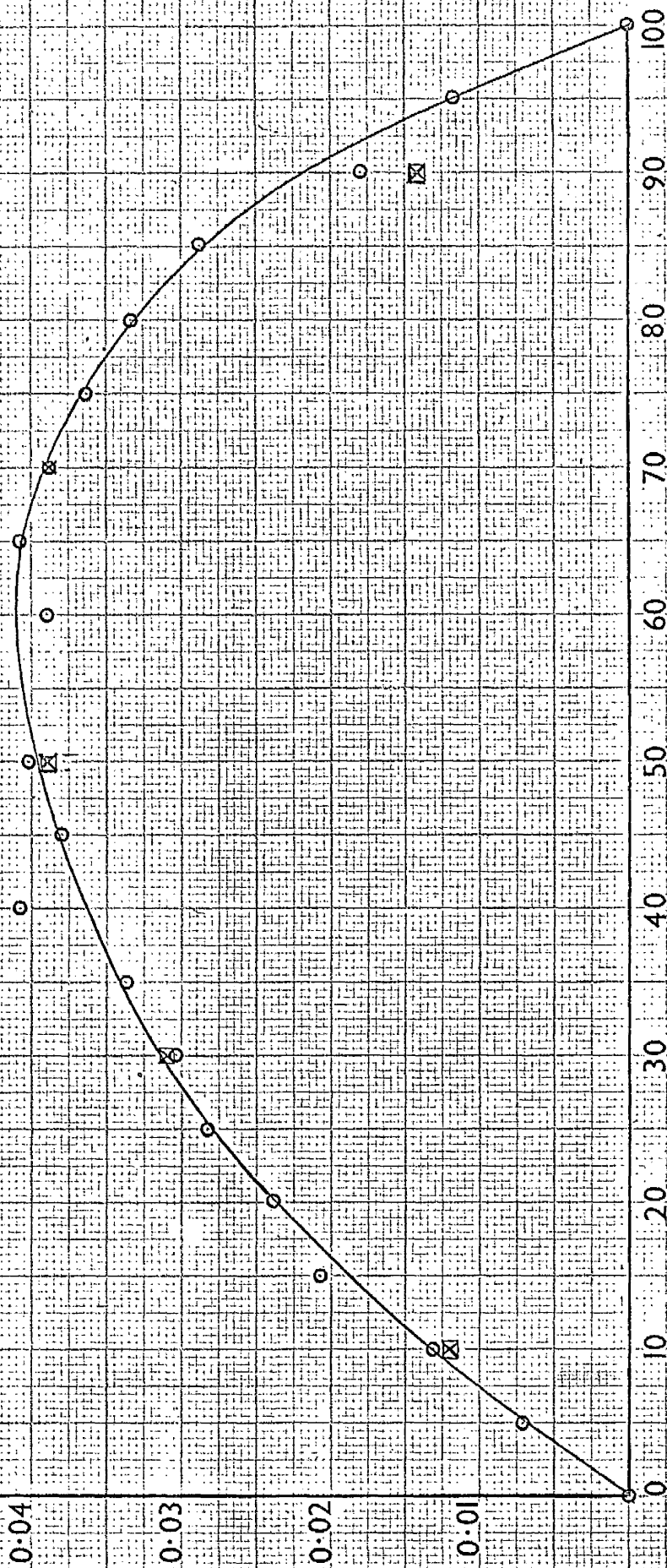


FIG. 10 LATTICE PARAMETER / COMPOSITION CURVE

present
G. F. DAY

% DEVN. FROM VEGARD'S LAW.



NICKEL. ATOMIC PER CENT.

FIG. II DEVIATION FROM VEGARD'S LAW.

SECTION 3.DENSITIES OF GOLD-NICKEL ALLOYS.

Table III lists the measured and theoretical densities at 25°C of gold-nickel alloys together with the percentage deviation from each other of these values,

$\frac{D_M - D_{TH}}{D_{TH}} \times 100$ (referred to hereafter as ΔD). For these

alloys ΔD is small and very close to zero. Indeed, within experimental error ΔD is effectively zero except in four cases. The alloys at 10 and 45 at.% nickel were reduced to a powder whose density agreed more closely with the theoretical density than did the original ingots. At 40 and 55 at.% nickel ΔD is positive corresponding to a larger measured than theoretical density.

The alloys at 40 and 55 at.% Ni. are those which are slightly above the curve of fig. 10. Since ΔD is positive coupled with the ostensibly high lattice parameter values, it is assumed that there had been an error in the made up compositions. Interpolation on the graph between 35 and 45 at.% nickel and between 50 and 60 at.% nickel shows that the compositions corresponding to the determined 'a' values are 39.5 and 54.6 at.% nickel. By using these compositions

TABLE II

DIMENSIONS OF GOLD-MERCURY ALLOY AT 25°C.

<u>At. % Hg.</u>	<u>Lattice Parameter (Å)</u>	<u>D_{111}</u>	<u>D_{11}</u>	<u>ΔD</u>
0	4.0784	19.325	-	-
5	4.0578	18.9321	18.9325	+0.002
10	4.0361	18.5388	18.4929	-0.14
15	4.0160	18.1078	18.0759	-0.08
20	3.9914	17.7206	17.6929	-0.02
25	3.9679	17.3003	17.3017	+0.01
30	3.9426	16.8843	16.8793	-0.03
35	3.9184	16.4339	16.4357	+0.01
40	3.8975	15.9847	15.9762	-0.449
45	3.8670	15.5354	15.4656	-0.15
50	3.8411	15.0880	15.0115	-0.05
55	3.8169	14.6514	14.5148	-0.432
60	3.7847	13.9913	13.9987	+0.04
65	3.7586	13.4177	13.4099	-0.06
70	3.7290	12.8519	12.8360	-0.06
75	3.6989	12.2562	12.2655	+0.04
80	3.6653	11.6075	11.6156	+0.05
85	3.6360	10.9902	10.9811	-0.08
90	3.5980	10.3534	10.3491	-0.04
95	3.5630	9.7456	9.7528	+0.13
100	3.5239	8.9162	8.9158	0.00

to determine the theoretical densities, the value of ΔD became negative and zero within experimental error. Analysis by cupellation is not sufficiently accurate to determine differences in composition to ± 0.5 at.%. Such interpolations of lattice parameter values are felt to be justified in the present case. Consideration of all evidence of the results for these two alloys leads to the conclusion that some human error has occurred during the handling of the component metals in the making up of these alloys.

On account of the experimental error in the volume of the specimens, the absolute concentration of vacancies cannot be established, but the measure of ΔD which is a direct indication of the number of vacancies present is in no instance of the same order as any values quoted by Ellwood and Bagley.¹¹ The present results are in agreement with Bay that there is no excess concentration of vacancies in gold-nickel alloys at 900°C.

SECTION 4.ACCURACY OF RESULTS.COMPOSITIONS OF THE ALLOYS.

The gold and nickel used in this investigation were of 99.99% and 99.999% purity respectively. It is conceivable that some loss of material could have occurred ^{during} melting through losses ^{by} evaporation should the melt have been held for a long period at temperatures above the liquidus. Table III shows the vapour pressures of the liquid metals.

TABLE III

<u>°C</u>	<u>V.p. of Au (mm.Hg.)</u>	<u>V.p. of Ni (mm. Hg.)</u>
1100	1.6×10^{-5}	-
1200	1.26×10^{-4}	-
1300	7.8×10^{-4}	-
1400	4.2×10^{-3}	-
1500	1.69×10^{-2}	1.17×10^{-2}

The loss in weight after melting was determined in every instance and was never greater than 0.1 at., which corresponds to an error in the lattice parameter values of 0.0005 Å. This error is too small to affect the purpose of the investigation.

Following the example of other investigators¹¹⁶¹ the final composition

was taken to be the composition as made up originally.

For the two alloys 40 and 55 at.-% nickel discussed in Section 3 it must be concluded that some human error took place during the making up of the component quantities of gold and nickel because the weight loss in melting was of the same order as the other alloys.

HOMOGENEITY OF THE INGOTS.

Lattice parameters measured from different parts of the ingots were found to agree to within ± 0.0002 Kx, proving the presence of homogeneous solid solutions.

ERROR IN THE VOLUME OF THE INGOTS.

The error in the volume of an ingot is governed by the error in the volume of the bottle ($\pm 0.002 \text{ ml}^3$). For volumes of the order of $0.2-0.3 \text{ ml}^3$ this corresponds to an error of roughly 1 part in 1000 or 0.1% which causes an error in density of less than 0.1%. This error, however, does mean that the absolute error in ΔD is $\pm 100\%$.

The advantage of the present method of volume determination is that the specimen is under vacuum prior to the entry of benzyl alcohol, and pumping continued until no gases are being evolved. Therefore, it is believed that no errors in volume could arise from air held in surface pores or microcracks.

POROSITY ARISING FROM INCLUDED GASES AND SOLIDIFICATION SHRINKAGE CAVITIES.

It was intended that all included gases in the as received metals would be removed by melting, solidification and re-melting under vacuum. The higher the temperature to which the melt was taken, the greater the degree of expulsion of occluded gases. Micro examination of the alloys of high gold content (60—95 at.-%) revealed shrinkage cavities. As explained in Chapter 3, section 5, the shrinkage porosity was drilled out with noticeable effects (Table IV)

TABLE IV.

<u>Atomic % Au.</u>	<u>ΔD (before drilling)</u>	<u>ΔD (after drilling)</u>
95	- 0.5	+ 0.002
90	- 0.8	- 0.25
85	- 3.0	- 0.17
80	- 0.32	- 0.12
60	- 1.2	- 0.19

TEMPERATURE OF BENZYL ALCOHOL.

The temperature of the benzyl alcohol was read to the nearest 0.1°C. Calculations showed that an error in temperature of more than 0.1°C could have a considerable effect on the measured density values. The error, however, would have needed to be very large to give values of ΔD of the order
 " reported by Hillwood and Dagley.

LATTICE IMPERFECTIONS.

Lattice imperfections such as dislocations and mosaic structures do cause some diminution of the measured density compared to the theoretical density but the effect is very small and essentially may be ignored.

VACANT LATTICE SITES.

Density measurements do not distinguish between single vacant lattice sites, multivacancies and porosity. For metals near their melting points the equilibrium concentration of vacant lattice sites is of the order of 1 site in 10000 atoms or 0.01%. Hence, the effect may be ignored.

CHAPTER 5.

DISCUSSION.

The results of the present investigation show that the gold-nickel system at 900°C does not have at any composition a concentration of vacant lattice sites in excess of that required for thermal equilibrium. No defect structures exist owing to the production of vacancies at Brillouin Zone overlaps. In contrast to the previous work of Ellwood and Bagley,¹¹ the lattice parameters of the system display a smooth variation with composition. The unit cell dimensions agree closely with those of Day and Kubaschowski¹² and Ebert.¹⁰ It can be reasoned that the results of Ellwood and Bagley¹¹ are in error because of surface concentration changes by deposition of atoms from the vapour phase during annealing of their alloys. The author suggests that had these investigators removed a substantial layer of metal from their ingots, the lattice parameter values obtained from the deeper layers would have been in agreement with the present findings.

The gold-nickel system manifests a large positive deviation from Vegard's Law. Such an effect is in keeping with the magnitude of the strain energy in the lattice as reported from thermodynamic investigations.

A very small concentration of vacancies is reported although the density method does not allow an accurate assessment of the absolute vacancy concentration. The error in the volume of the density bottle is 2 parts in 30,000 which when applied to the alloy gives an error of 2 parts in 2,000 - 3,000. This error could be reduced by decreasing the volume ratio of bottle to specimen which in the present case was about 10 : 1. Under such circumstances it would be possible to plot ΔD against composition and determine whether or not the contours of the graph obtained, corresponded to the heights of the intervals between liquidus and solidus. If such a relationship were to exist, the deviations between observed and theoretical densities could be attributed to solidification microporosity.

//

The density values of Ellwood and Bagley must be ignored since in the first instance their theoretical densities are in error because of the errors in lattice parameter values. However, most of their reported lattice dimensions are larger than the present values which would decrease D_{TH} and hence ΔD . It is proposed that their specimens had low measured densities because of shrinkage cavities such as are reported for five specimens in the present work. Moreover, in view of the reported

reaction between $C - SiO_2$ and $C - Al_2O_3$, it is probable that ⁵² Ellwood and Bagley did not have a good vacuum in their system. This failing would be expected to hinder the outgassing of the molten alloys.

The present findings are in agreement with the conclusions drawn from work on other systems, $Al - Sn$, $Al - Mg$ ⁴¹ and $Sb - Sn$. ^{43,44} To date, no such system appears to display defect structures arising from energy considerations in Brillouin zone overlaps. Any differences between theoretical and measured densities are probably due to solidification microporosity. To confirm this postulate, alloys could be prepared by vapour diffusion techniques as reported by Holtrich and Dodd for an $Al - Sn$ alloy. ⁴¹ No microporosity would be expected in this case.

⁶² It has been reported from a further investigation of $Mg - Al$, and $Mg - Cd$ that no sharp change in 'c' spacings with composition occurs. $Mg - In$, however, when re-investigated did as previously reported, show an anomalous 'c' spacing variation. ^{32,33} The investigations of these systems by Raynor and Hume-Rothery and Raynor ^{34,36} were thought to be definitive works on the experimental observation of lattice dimensional changes arising from Brillouin zone effects. If the recent work on magnesium systems is proved to have reported correct 'c' spacing values, then it must be concluded that for all alloy systems,

whether or not vacant lattice sites are formed, lattice parameter data provide an unsatisfactory tool with which to detect the initial stages of Brillouin Zone overlaps.

PART II

SELF-DIFFUSION OF GOLD IN NICKEL.

INTRODUCTION.

The conclusion which has been drawn that the gold-nickel system does not at any concentration contain an excess number of vacant lattice sites renders a diffusion investigation specifically as planned much less useful. As the theory of diffusion has progressed, several studies have been made on the diffusion aspects of the gold-nickel system and the results have been reported with reference to the contemporaneous state of theory.

The attention of research workers has recently been concentrated on the atomic mechanisms of diffusion, a field of study which has progressed with the advent of the use of radioactive tracers. Although many postulates have been forwarded which have found confirmation in experiment, the theory is sufficiently incomplete as to benefit considerably from any new accurate data. Hence, it seemed justifiable to carry out some investigation of the rates of diffusion of tracer quantities of gold in nickel. It was, moreover, challenging to attempt such a task under conditions which are thought to obviate some of the accepted experimental difficulties and for which no previous data was available.

Part II describes the determination of the self-penetration of an infinitely thin layer of gold into a cylinder of nickel by the measurement of the diffusion coefficient of gold in nickel by the measurement of the penetration of nickel. For the diffusion times employed the penetration of

gold occurs to a depth of only .02 of the cylinder radius and over this very shallow depth radial effects are neglected in the mathematical analysis employed. The experimental advantage of using a cylinder of nickel lies in the ease with which sections can be taken by turning the cylinder on an ordinary lathe and by monitoring the penetration distance with a standard micrometer. For unidimensional diffusion into the end face of a cylinder, the experimental technique of penetration analysis requires more elaborate apparatus.

CHAPTER 1.

SECTION 1.

MATHEMATICS OF DIFFUSION.

The established approach to a mathematical rationalisation of diffusion phenomena as forwarded initially by Adolf Pick, has been justified on account of its general applicability and by its freedom from any assumptions regarding the mechanism of transference involved. In addition, the extensions of Pick's Laws by later workers to account for phenomenological observations have shown very close agreement between theory and experiment.

Pick's First Law states that the flow or flux J of a substance diffusing through unit area of a medium is directly proportional to the concentration gradient of that substance i.e.

$$J_1 = -D_1 \left(\frac{\partial c_1}{\partial x} \right)_t \quad \text{--- (1)}$$

where D is a proportionality constant termed the diffusion coefficient of substance 1 and has the dimensions (length²/time). Equation (1) is operative under the conditions of a steady state when $\left(\frac{\partial c}{\partial t} \right)_x = 0$ since it is only then that a time invariant concentration gradient exists in a medium. Pick's first law has been applied to the "quasi-stationary" state to obtain D values for the diffusion of gases or solutes through a membrane.

It is difficult to devise an experiment which would afford the determination of D for one metal in another under

the conditions of a steady state. If a steady state does not exist, then the concentration of diffusing substance at any point must change with time i.e. $(\frac{\partial c}{\partial t})_x \neq 0$. For the case of diffusion in the x-direction only, the flux difference between two planes (1) and (2) a distance dx apart can be related by

$$J_1 = J_2 - dx \frac{\partial J}{\partial x} \quad \text{--- (2)}$$

which leads to a second order differential equation since equation (2) implies that the concentration of diffusing element in the volume $1. dx \text{ cm}^2$ is being altered with time. If the change in concentration is expressed by $\frac{dc}{dt}$ then the change in concentration in the volume between planes (1) and (2) is

$$J_1 - J_2 = dx \frac{\partial c}{\partial t} = - dx \frac{\partial J}{\partial x}$$

When $dx \rightarrow 0$ equation (1) is valid even although the concentration at that point is changing with time.

Therefore:

$$\begin{aligned} dx \cdot \frac{\partial c}{\partial t} &= dx \frac{\partial}{\partial x} \left(D \frac{\partial c}{\partial x} \right) \\ \text{i.e.} \quad \frac{\partial c}{\partial t} &= \frac{\partial}{\partial x} \left(D \frac{\partial c}{\partial x} \right) \quad \text{--- (3)} \end{aligned}$$

Equation (3) is the statement of Fick's Second Law when D varies with penetration distance or more strictly when D varies with concentration.

When D is constant for all x then,

$$\frac{\partial c}{\partial t} = D \left(\frac{\partial^2 c}{\partial x^2} \right) \text{ --- (4)}$$

The solutions to equation (4) for various co-ordinate systems and boundary conditions are given in standard reference works such as Carslaw and Jaeger² and Crank.³

THE INSTANTANEOUS SOURCE SOLUTION.

This solution to Fick's Second Law has been used extensively to determine the self-diffusion coefficient for metals and the diffusion coefficient for one metal in another by the use of radioactive tracers. The method essentially involves diffusion at infinite dilution when D is constant for all x where diffusion occurs in the x direction only.

If a thin film of solute is sandwiched between the end faces of two cylinders of solvent metal and diffusion of solute is allowed to occur, then the variation of solute along the length of the cylinders is given by.

$$C = \frac{C_0}{2(\pi Dt)^{\frac{1}{2}}} \exp. \left(\frac{-x^2}{4Dt} \right) \text{ --- (5)}$$

where C_0 is the initial concentration of solute. The plane $x = 0$ is the plane at which the solute is concentrated at $t = 0$. Hence, equation (5) for $t > 0$ describes diffusion in the directions of positive and negative x . Substitution of the

equation into equation (4) shows that it is indeed a solution to the second law. Moreover, equation (5) is symmetrical with respect to x and for $t = 0$ the equation vanishes except where $x = 0$ and so satisfies the boundary conditions of the problem which are

$$|x| > 0 \text{ for } c \rightarrow 0 \text{ as } t \rightarrow 0$$

$$\text{and } x = 0 \text{ for } c \rightarrow \infty \text{ as } t \rightarrow 0$$

while for all t the quantity of solute remains constant

$$\text{i.e. } C_0 = \int_{-\infty}^{+\infty} c dx$$

which must be the case because of the law of conservation of mass. The study of equation (5) shows that $\frac{dc}{dx} = 0$ at $x = 0$ and hence the flux across this plane is zero.

Equation (5) is the solution for a thin film of solute in the middle of an infinite bar. For practical purposes the case of the semi-infinite bar is more useful. Provided that the bar is sufficiently long that the solute does not reach the end of the bar and undergo reflection, then the equation is still valid.

If a similar infinitely thin layer of solute is formed on the face of a bar, the situation presented is the same as above except that the bar has to be cut at the plane $x = 0$. Diffusion can now occur in the direction of positive x only, all of the negative x movement being reflected at $x = 0$. Assuming that no solute is lost

by evaporation, then the plane $x = 0$ is impermeable and the solution is

$$C = \frac{C_0}{(\pi Dt)^{\frac{1}{2}}} \exp. - \frac{x^2}{4Dt} \quad \text{--- (6)}$$

where C at any x is twice that given by equation (5) since diffusion occurs in one direction only. Clearly, the property of the original solution that $\frac{dC}{dx} = 0$ for $x = 0$ is unchanged by the reflection at $x = 0$ i.e. the flux is zero at the plane $x = 0$.

To determine D , a thin film of solute, usually radioactive, is plated or vapourised onto the face of a semi-infinite bar and diffusion is allowed to occur. At the end of the diffusion anneal the concentrations are determined of successive thin sections from planes parallel to the face. Equation (6) shows that a plot of $\ln C$ against x^2 is a straight line of slope $(4Dt)^{-1}$ and if t is known D can be easily calculated.

D is termed the self-diffusion coefficient of a metal when the thin film is a radioactive layer of that metal. On the other hand, the thin film may be that of a solute which diffuses at infinite dilution in the solvent, in which case D is termed the self-diffusion coefficient of the solute in the solvent.

The importance of D measurements by the thin film technique arises because a tool is thereby provided to allow an

elucidation of the mechanisms of atom movements and of the effects of small quantities of impurities on the atomic array of the solvent. It has also been shown that the thin film D values can be related to the bulk diffusion or chemical diffusion coefficient of one metallic phase in another.

THE SOLUTION FOR VARIABLE D .

When D is not constant but varies with concentration, the D ^{value} varies with position along the specimen. Matano ⁴ has applied the mathematics of Boltzmann ⁵ to provide a solution to this problem where $D = D(c)$ and has shown that for a concentration C_1 at some point of penetration,

$$D(C_1) = - \frac{1}{2t} \left(\frac{dx}{dc} \right)_{C_1} \int_{C_0}^{C_1} x dx \quad \text{--- (7)}$$

The use of this equation has been demonstrated amply by Rhines and Mehl. ⁶ D obtained from equation (7) is referred to as the chemical diffusion coefficient D_{chem} or \tilde{D} . In itself \tilde{D} is meaningless and is really only a measure of the rate of homogenisation.

Smigelskas and Kirkendall ⁷ have demonstrated that for a diffusion couple, the flux of atoms of one element can be appreciably greater than the flux of the other across the same plane. Darken ⁸ has analysed this phenomenon and has shown that for components (1) and (2) that

$$\tilde{D} = D_1 N_2 + D_2 N_1 \quad \text{--- (8)}$$

where D_1 and D_2 are determined from the rate of movement of inert markers sited in the diffusion couple. Furthermore, from thermodynamic considerations, Darken⁸ also showed the diffusion coefficient D_1^* for a tracer quantity of element (1) in an alloy of composition N_1 can be related to D_1 by

$$D_1 = D_1^* \left(1 + \frac{d \ln \chi_1}{d \ln N_1} \right) \quad \text{--- (9)}$$

and hence

$$D = (D_1^* N_2 + D_2^* N_1) \left(1 + \frac{d \ln \chi_1}{d \ln N_1} \right) \quad \text{--- (10)}$$

The accuracy of this relationship has been demonstrated⁹ for Cu-Zn and by Reynolds et al³⁴ in a study of the gold-nickel system.

MECHANISMS OF DIFFUSION.

From considerations of the properties of an atomic lattice and the relative sizes of atoms of the elements, several mechanisms have been postulated to account for diffusion in metals. Diffusion can occur along grain boundaries, along external surfaces and through the bulk of the solid. The latter is generally referred to as volume diffusion and is the most important process in practice because grain boundaries and other so called short circuiting paths, e.g. dislocation lines, comprise a very small portion of the bulk of the metal.

1. VACANCY MECHANISM.

In part 1, it has been shown that all metals contain an equilibrium concentration of vacancies. When an atom undergoes translational movement by jumping into a vacant site, the atom is said to have diffused by a vacancy mechanism. This type of process has been established as the predominant one for substitutional diffusion in close packed metallic phases. The energy barrier for the movement of an atom into a vacancy is the energy of distortion required to move momentarily apart the atoms on the other sites proximate to the vacancy. In this instance the energy required is relatively small and consequently atomic movement is not prohibitively retarded.

2. INTERSTITIAL MECHANISM.

An interstitial mechanism operates when an atom diffuses by moving from an interstitial site to one of its nearest neighbour interstitial sites without causing permanent displacement of the matrix atoms. This mechanism probably operates in the case of the diffusion of atoms which in alloy phases normally occupy interstitial positions e.g. carbon or nitrogen in iron. Before the atom can move there must occur a local dilation of the lattice which allows the atom to pass through to its new position. If the atoms of the phase are of comparable size the distortional energy required becomes excessive, so that an interstitial mechanism must effectively cease to operate.

3. RING MECHANISM.

The large distortion of the lattice which must occur should diffusion take place by the direct interchange of two neighbouring atoms renders such a mechanism extremely improbable. Zener,¹⁰ however, has proposed that direct interchange is merely a limiting case of diffusion by a synchronised cyclic motion of a number of atoms and that a ring movement of 4 atoms has a lower potential energy barrier than a two atom exchange. The lattice distortion involved in a three or four atom ring mechanism is considerably smaller than in direct exchange. From statistical mechanical considerations of the kinetics of diffusion in cubic

metals, Pound et al,¹¹ have reasoned that diffusion by a four atom ring mechanism may occur in pure chromium and uranium in which the structures are the relatively open body centered cubic.

4. RELAXATION MECHANISM

12

It has been postulated for diffusion in solid metals that the diffusing atom may move within small regions of disorder extending over 12 - 14 atoms. These atoms are considered to relax inwardly around lattice vacancies and the energy content of the region is similar to that of the equivalent number of atoms in the liquid state. Thus the diffusion atoms are imagined to move freely in a liquid like region which itself moves by a process analogous to local melting and freezing.

ATOMIC THEORY OF DIFFUSION.

Atoms diffusing in a crystal lattice are subject to various restrictions on their movements. Assuming, however, that such factors can be ignored, the diffusion coefficient D for atoms moving in one dimension only between two planes can be related to the frequency, $\sqrt{\quad}$ times per second, with which an atom jumps from one plane to another and to the jump distance α . If there are n_1 diffusing atoms in plane 1 and n_2 diffusing atoms in plane 2, ($n_1 > n_2$) then the net flux per unit area from plane 1 to plane 2 is:

$$J = \frac{\text{number of atoms}}{(\text{area}) (\text{time})} = \frac{\frac{1}{2} n_1 \sqrt{\quad} \delta t - \frac{1}{2} n_2 \sqrt{\quad} \delta t}{(1) (\delta t)}$$

$$= \frac{1}{2} (n_1 - n_2) \sqrt{\quad}$$

Since $C_1 = \frac{n_1}{\alpha^2}$ and $C_2 = \frac{n_2}{\alpha^2}$ then,

$$J = \frac{1}{2} (C_1 - C_2) \alpha \sqrt{\quad}$$

Considering that C changes slowly enough with composition that

$$C_1 - C_2 = -\alpha \frac{\partial C}{\partial y}$$

and so

$$J = -\frac{1}{2} \alpha^2 \sqrt{\quad} \frac{\partial C}{\partial y} \quad \text{--- (3.1)}$$

which is identical to Fick's first Law provided that

$$D = \frac{1}{2} \alpha^2 \sqrt{\quad} \quad \text{--- (3.2)}$$

If the further assumption is made that α is the interatomic spacing ($\sim 1\text{\AA}$) and taking $D = 10^{-8} \text{ cm}^2/\text{sec}$ which is the value for most close packed metals near the melting point, then $\sqrt{\tau} = 10^{-8} \text{ sec}^{-1/2}$. Since the vibrational or Debye frequency for such atoms is $10^{12} - 10^{13} \text{ sec}^{-1}$, then it is evident that in the simple case described here that each atom would change position only once in $10^4 - 10^5$ oscillations.

The "random walk" problem is concerned with estimating the distance which an atom will move from its position by a consideration of the randomness of the jump directions. For a three dimensional lattice face centre cubic lattice it can be shown that the average mean displacement R_n of the atoms from their original sites can be related to the individual jump distances τ by

$$R_n^2 = n\tau^2$$

where n is the number of jumps which have occurred. If as above τ is the jump distance then,

$$R_n^2 = n\alpha^2 = 6Dt.$$

Hence,

$$D = \frac{1}{6} \alpha^2 \tau^{-1} \quad (3.3)$$

D in this case differs by a factor of three from that given previously because diffusion is now considered to be in three dimensions.

It is possible to determine the factors which govern the magnitude of D in the case of self-diffusion in cubic metals by a vacancy mechanism provided that certain simplifying assumptions are made regarding the indistinguishability of the behaviour of the different isotopes of a pure metal. The number of jumps which each atom makes is dependent upon the number of nearest neighbours, the probability p_v that nearest neighbour sites is vacant and the probability that the tracer atom may jump into a vacancy. Shownon¹³ derives the equation

$$D = a_0^2 p_v w$$

where a_0 is the lattice parameter of the metal and w is the jump frequency of ^{an} atom into a vacancy. Since for a pure metal the probability of a vacancy being a nearest neighbour is equal to the equilibrium fraction of vacant sites present N_v , then

$$D = a_0^2 N_v w \dots \dots \dots (3.4)$$

This equation demonstrates the factors which determine D and thus the rate of movement of atoms in a close packed lattice.

EFFECT OF TEMPERATURE ON DIFFUSION.

Increase of temperature increases the jump frequency factor and thus increases D . It is found experimentally that a plot of $\ln D$ versus T^{-1} is a straight line

or that

$$D = D_0 \exp. - \frac{Q}{RT} \quad \dots \dots (3.5)$$

D_0 termed the frequency factor, and Q , the activation energy for diffusion are determined from the graph. Both D_0 and Q are temperature independent.

IMPURITY DIFFUSION IN PURE METALS.

Experimentation has shown that the self-diffusion coefficient for tracer quantation of impurity atoms in a solvent may differ considerably from the self-diffusion coefficient of the solvent. Attempts to rationalise this phenomenon are based on the study of the extent to which the electronic or valence differences on the one hand and the size differences on the other between the solute and solvent atoms can effectively alter:-

- (1) the factor w of equation (3.4)
- (2) the probability that a nearest neighbour site is vacant.

14

Laxerius has treated this problem by ignoring the size differences and concentrating only on the valence differences Z between solute and solvent. For the case where $Z > 0$ the electronic differences cause the electron charge density to be increased around the solute atom on account of the electrostatic attraction between the impurity and the electron gas resulting in a 'screening' of the solute atom. If a vacancy is formed

next to a solute occupied site then its original charge of $-e$ (where the solvent is univalent) interacts with the electrostatic potential around the solute atom to reduce the energy of the vacancy. Thus the overall effect is to increase the probability of a vacancy becoming a nearest neighbour of the solute atom i.e. $p_v > N_v$. In addition, there is a force $e (dV/dr)$ where

V = electrostatic potential around the impurity atom,

r = radial distance from the impurity atom.

which tends to attract the impurity atoms to the vacancies. The overall result, therefore, on the diffusion process is that the movement of the solute is limited by the factor of the rate of exchange of the solvent atoms with vacancies.

The effects of size differences between atoms have been considered by Swalin¹⁵ whose treatment assumes that the solute atom is compressible and that the lattice is an elastic continuum. Any alteration in the energy of diffusion as compared to solvent self-diffusion is then dependent upon the elastic strain in the lattice brought about ^{by} the diffusing solute. There are many assumptions implied in this approach but empirical results¹⁶ show that the concepts involved are partially valid.

CONCENTRATION EFFECTS.

17

It has been pointed out that many mechanisms impose restrictions on the successive jumps of atoms, so that any

theoretical treatment of diffusion which assumes random jumps of atoms is invalid. There is in theory a correlation between successive jumps which reduces the degree of randomness of atomic movement. For self-diffusion in close packed metallic phases, to a first approximation

$$D = f \frac{2}{3} D_0 \quad (18)$$

where f is the correlation factor and is close to unity.

For impurity diffusion¹⁹ there is, in addition to the normal correlation effects of the solvent atoms and impurity atoms, the electrostatic attraction between solute atoms and vacancies which increases the correlation between successive vacancy jumps. Hence, $f \ll 1$ and a measure of its relative effect with various solutes in nickel could be determined by the experimental procedure to determine D values described in a later chapter.

GRAIN BOUNDARY AND VOLUME DIFFUSION.

As a result of the short circuiting behaviour of grain boundaries for diffusing atoms, the rates of diffusion in single crystals usually differ markedly from that in polycrystalline materials. ²⁰ The mean jump frequency of atoms in grain boundary regions is higher than in the matrix and consequently the diffusion coefficient is larger. ²⁰ It has been found by experiment that at higher temperatures close to the melting point the differences in atomic jump frequency of atoms in the two regions is so small as to eliminate any observable effect of grain boundary diffusion while at lower temperatures grain boundary diffusion is predominant.

²¹ Fisher has analysed the effects of grain boundaries on diffusion and has been able to demonstrate, allowing certain assumptions, that the plot of $\ln c$ against x after an annealing time t is a straight line of slope:

$$-\frac{1}{2} \frac{D_B}{D_L t} \left(\frac{\delta D_B}{D_L} \right)^{\frac{1}{2}}$$

where D_L is the volume diffusion coefficient, D_B is the grain boundary diffusion coefficient and δ is the thickness of the grain boundary.

22

A further analysis by Whipple introduces a factor:

$$\beta = \frac{D_B \delta}{2D_L (D_L t)^{\frac{1}{2}}}$$

whose value can be used to predict the conditions under which grain boundary diffusion is significant. Grain boundary diffusion distorts the lateral (i.e., perpendicular to x) concentration contours. The value of D_g/D_L can be calculated which will show this effect at any concentration where $C = \text{fraction of } C_0$.

In the course of the present investigation it was necessary to study diffusion in a single crystal of nickel. Experimental results have been reported that where grain boundary diffusion is effective, the plot of $\ln C$ versus x^2 is linear at first but then deviates from linearity into a curve. An accurate determination of a value D can be made from the linear portion of the graph. However, as the work of Wajda²³ demonstrates, this diffusion coefficient does not agree with the value obtained from extrapolation from higher temperatures where the diffusion coefficient obtained is the true D_L under the conditions of the experiment. At the higher temperatures volume diffusion masks any grain boundary effects. Therefore, it is unlikely that any worthwhile value of D_L can be obtained where the rate of diffusion in grain boundaries is excessive compared to the rate of diffusion in the bulk of the metal.

CHAPTER 2.

SECTION 1.

RADIOACTIVATION ANALYSIS.

When diffusion coefficients are determined by thin film techniques it is standard procedure to plate or evaporate radioactive material onto the surface of a solvent. The concentration at various layers after annealing is then determined as the number of counts per unit weight per unit time. However, the deposition technique described later does not lend itself to the use of radioactive gold. Therefore, the penetration curve had to be determined by activating the sections from the annealed specimen in a flux of neutrons and then measuring the rate of decay of the product. The technique of radioactivation analysis is based on the formation of radioactive nuclides as a result of reactions between the nuclear particles and the isotopes of the element under investigation. For the most part, two particle reactions are utilized, one particle being the reactant (proton, neutron, deuteron, alpha particle) and the other being the product.

RADIOACTIVE DECAY.

Radioactive decay is a purely random process and the rate at which radioactive nuclides decay is dependent solely on the number present at the time, i.e.

$$\frac{dN}{dt} = -\lambda N \quad - - - - - (1)$$

N = number of radioactive nuclei present at time t .

λ = the radioactive disintegration constant and is characteristic of the radioactive isotope under consideration.

Integration of (1) gives:

$$N = N_0 \exp. - \lambda t. \quad \dots (2)$$

where N_0 = number of radioactive atoms present at $t = 0$.

The half-life $t_{\frac{1}{2}}$ of an isotope is the time taken for half of the original radioactive material to decay i.e.

$$\frac{1}{2} N_0 = N_0 \exp. - \lambda t_{\frac{1}{2}}$$

$$\ln 2 = \lambda t_{\frac{1}{2}}$$

$$t_{\frac{1}{2}} = \frac{0.693}{\lambda}$$

Hence, $t_{\frac{1}{2}}$ is a nuclear constant.

PRODUCTION OF RADIOISOTOPIES.

The rate of accumulation of an isotope is given by the rate of production R_p minus the rate of decay during production.

$$\frac{dN}{dt} = R_p - \lambda N \quad \dots (3)$$

Integration of (3) gives.

$$N = \frac{R_p}{\lambda} (1 - \exp. - \lambda t) + N_0 \exp. - \lambda t.$$

where N_0 is the number of radioactive nuclei present originally and is normally zero. Therefore,

$$N = \frac{R_p}{\lambda} (1 - \exp. - \lambda t.)$$

The rate of disintegration of activated nuclei is

$$R_G = N \lambda = R_P (1 - \exp. - \lambda t) \dots (4)$$

RADIOACTIVATION ANALYSIS IN A NEUTRON FLUX

The rate of activation of an isotope in a particular sample is proportional to the intensity of the neutron flux, the concentration of target nuclide present, and the nuclear capture cross-section for the particular neutron-nucleus reaction. This latter quantity is broadly speaking, a measure of the probability that the particular nucleus will capture a neutron.

$$R_P = \phi n \sigma = \frac{\phi m N^0 f \sigma}{M} \dots (5)$$

ϕ = neutron flux in neutrons/cm²/sec.

n = number of target nuclides.

m = mass of the trace element in the sample.

M = atomic weight of the trace element.

f = fractional isotopic abundance of the target nuclide.

N^0 = Avogadro's number = 6.023×10^{23} atoms/gram-atom.

σ = reaction cross section (cm²/atom) 1 barn = 10^{-24} cm²

Therefore:
$$R_G = \frac{\phi m N^0 f \sigma}{M} (1 - \exp. - \lambda t)$$

Thus the concentration of element in a particular sample can be determined as R_G .

When more than one of the elements in a particular sample have half-lives relatively close to each other, the

element under examination must be separated by radiochemical separation. Table I shows the properties of the isotopes of gold and nickel which are produced by neutron reactions.²⁵

TABLE I

Isotopo <small>PRODUCED BY NEUTRON REACTIONS</small>	P_0 <small>PERCENT</small>	Product <small>PRODUCED BY NEUTRON REACTIONS</small>	$t_{1/2}$ <small>HOURS</small>
Au ¹⁹⁷	100	Au ¹⁹⁸ +	2.70 days
Ni ⁶²	3.66	Ni ⁶³ +	125 years
Ni ⁶⁴	1.16	Ni ⁶⁵ +	2.56 hours

It can be seen that Ni⁶⁵ will be almost inactive before the half-life of Au¹⁹⁸ is reached. Therefore, if the samples are counted about 25 hours after irradiation (i.e. $10 \times t_{1/2}$ for Ni⁶⁵), the rate of disintegration determined is that of Au¹⁹⁸ only. Radiochemical separation was, therefore, unnecessary.

SECTION 2.GAMMA SCINTILLATION SPECTROMETRY.

Gamma scintillation spectrometers were used in the present investigation to determine the presence of minute quantities of impurities in powders of nickel. The technique can be described as the nuclear analogue of light spectrometry because a γ ray energy is characteristic of a particular radioisotope and the counting rate associated with it is proportional to the quantity of the isotope present.

Gamma radiation reacts with matter and transmits its energy to the electrons to free the electrons from their nuclei. This stream of electrons is produced by three effects.

(1) The Compton effect

(2) The photoelectric effect

(3) Pair production in which the γ photon interacts with the Coulomb field surrounding a nucleus or an electron to produce a positron-electron pair. The positron later reacts with an electron to produce γ rays which may then undergo (1) and (2)

If the above interactions occur in a phosphor, the most efficient material being sodium iodide crystals, the subsequent de-excitation and recombination of the electrons converts their energies into light pulses or scintillations, the brightness of which is a measure of the total energy absorbed.

The light pulse is then converted within a standard apparatus into a measurable voltage pulse by a multistage photomultiplier and amplified by a linear amplifier.

A standard laboratory apparatus, a "Laben" 512 channel pulse height analyser was used to determine the spectrum for any sample. A single channel pulse height analyser passes only those pulses whose heights lie between fairly close limits as set by the controls of the instrument. In a multi-channel analyser, the channels are all adjacent and cover a continuous energy range. The count rates of the recorded pulses are proportional to the incident photon flux (i.e. the energy of the γ rays) and these count rates are automatically printed out. To determine the characteristic γ energy peak for the elements, two standard sources, Caesium¹³⁴ and Cobalt⁶⁰ are used. Within the energy range as set by the instrument, the channels on which are sited the γ energy peaks of these isotopes can be located. Thus the γ energy of any isotope under investigation is determined by dropping a perpendicular from the peaks of the channel number versus count rate plot onto the linear graph of the γ energies of the standards. The isotopes under investigation can then be identified from tables of γ energies.^{26,27}

CHAPTER 3.

1777

EXPERIMENTAL PROCEDURE.SECTION 1.DEPOSITION OF A THIN FILM OF GOLD.

Electroplating and vacuum electrodeposition are the two standard methods of forming a thin film of metal for diffusion experiments. For the present investigation it was necessary to choose a method which would allow a layer of gold of reasonably uniform thickness to be deposited on a cylinder of nickel. It has been shown that absolute uniformity is not²⁸ essential. In addition it was considered worthwhile to utilize a method which would eliminate the barrier effects to uniform diffusion of any oxide layer on the nickel. The presence of an oxide layer has been reported by Mykura²⁹ to be present on nickel heated under vacuum at 900°C.

It is probable that the immersion of nickel into an electroplating bath causes some surface reaction resulting in the formation of an impurity layer which would subsequently exist between the nickel and the deposited film of gold. On the other hand, by completely surrounding the nickel cylinder with a gold electrode, the deposition could be readily achieved.

Electrodeposition does not permit the oxide film formed in the atmosphere to be removed immediately prior to the

NOT TO SCALE

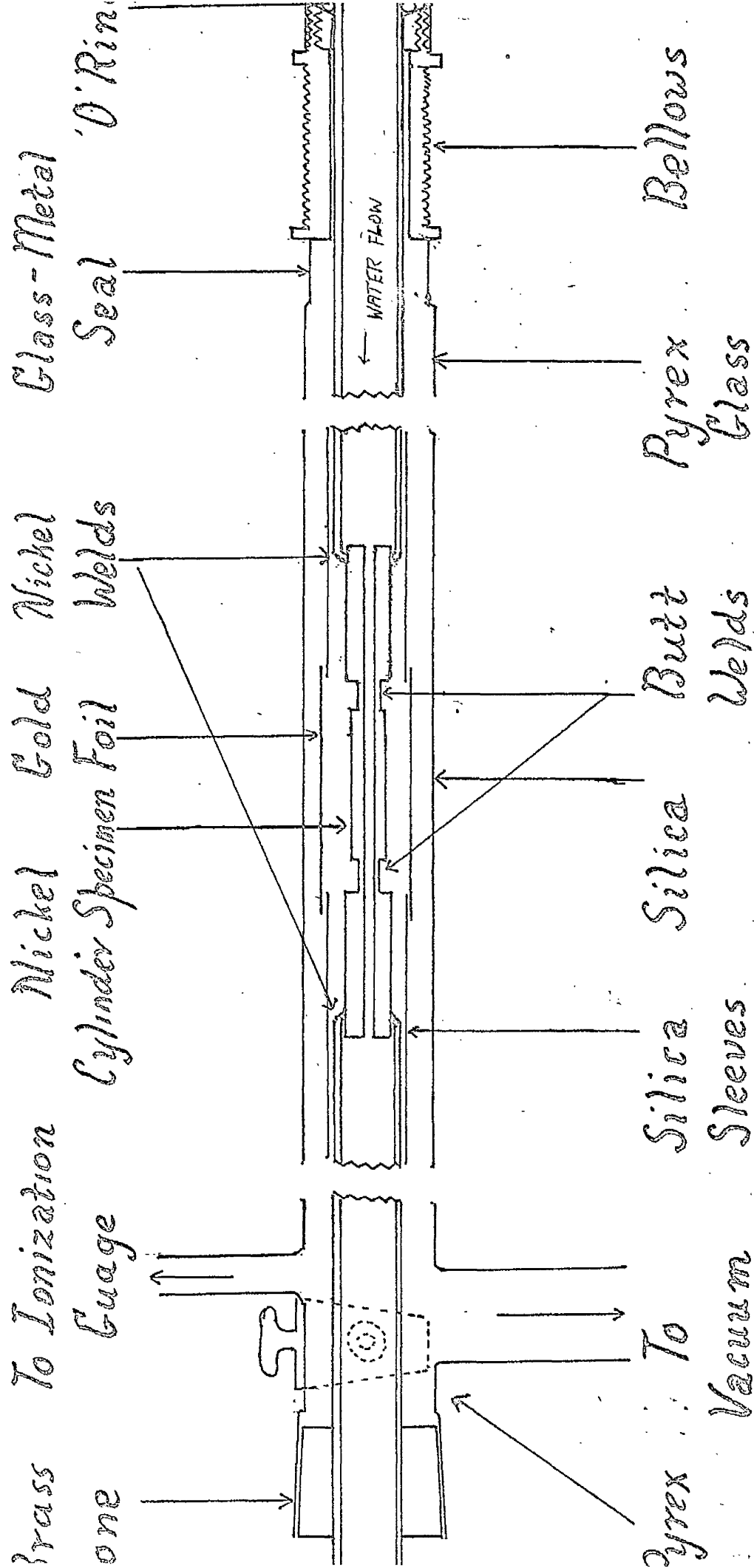


Fig. 1. Apparatus for Deposition of Gold Film.

deposition of gold. Moreover, a complex problem arises as to the manner in which a reasonably uniform layer might be produced on a cylindrical surface, by the use of any standard apparatus for vacuum electrodeposition.

The above considerations implied that to meet the requirements of the investigation a new method had to be evolved to deposit a gold film. After several attempts a method was evolved which in essence caused the distillation onto a cold nickel surface of gold vapour from a gold source at 900°C. The apparatus used is shown in figs. 1 and 2. A cylinder 5 cm. long of 99.999% purity nickel was machined to 0.9 cms. \pm 0.0005 cms. diameter, after which 0.5 cms. at each end was reduced to 0.5 cms. diameter. Along the axis

$\gamma = 0$ a hole 0.3 cms. diameter was bored. Two lengths of commercially pure nickel rod 1 cm. diameter were welded using nickel electrodes to two lengths of nickel tubing 1.2 cms. outside diameter and 2 m.m. wall thickness. The nickel rods which were reduced in section at their ends and bored in the same manner as the pure nickel cylinder were butt welded to the latter. Thus a flow of water could be maintained through the finely machined specimen to render its surface cool, despite the ambient temperatures. A brass fitting machined to the standard "Quickfit" B.29 dimensions cone joint was soldered to one of the nickel tubes.

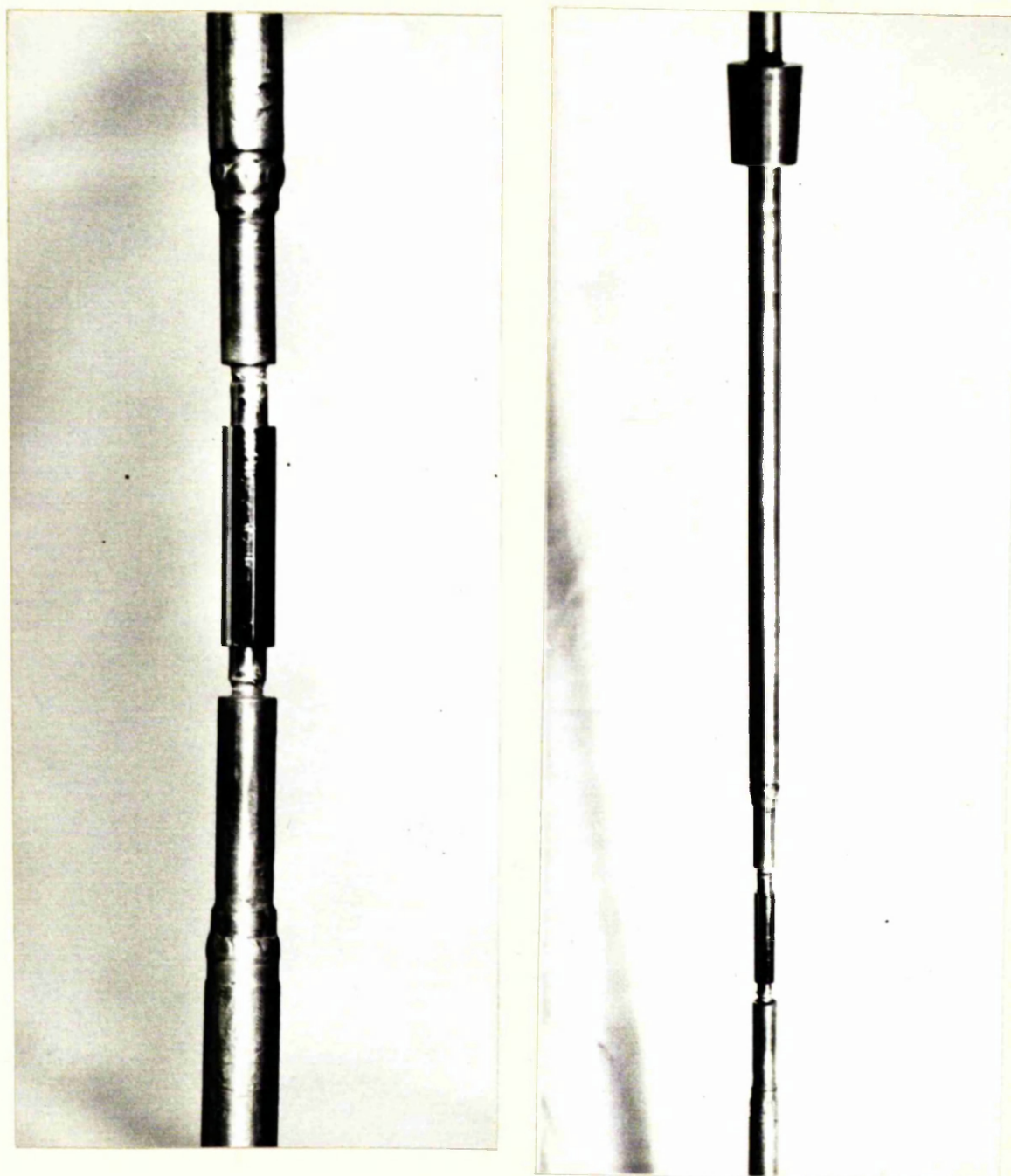


FIG. 2.

NICKEL CYLINDER IN POSITION PRIOR TO
INSERTION INTO THE DISTILLATION APPARATUS.

The entire assemblage was then inserted into a tube of pyrex-silica-pyrex lengths on one end of which was a metal-glass joint to which was soldered a bellows to accommodate the later expansion of the nickel. On the other glass section a vacuum stopcock, and ionisation valve and outlet to the evacuation system were attached. The brass cone was sealed in position by Apieson 'N' wax. A rubber 'O' ring was fitted around the nickel which protruded beyond the bellows and was pressed against the bellows to provide a vacuum tight seal.

The chamber was evacuated by a mercury diffusion pump backed by a rotary pump. To increase the efficiency of the system a liquid nitrogen trap, a glass trap and a phosphorus pentoxide trap which absorbs water vapour, were added.

Before being inserted into the evacuation chamber, the nickel assemblage was tested for air leaks by attaching it through rubber vacuum to a rotary pump. The nickel specimen was then taken to be electropolished *in situ*.

A length of gold foil was positioned around the nickel cylinder by fitting it around the ends of two silica sleeves which fitted over the commercially pure nickel rods and cylinders. Experimentation demonstrated that a more satisfactory deposit of gold could be obtained when the gold foil had been perforated.

The deposition chamber was evacuated down to 10^{-6} m.m. Hg. and flushed twice with hydrogen. A constant atmosphere of hydrogen was maintained thereafter at the stopcock by having the hydrogen from its source passing via a 'T' junction into a column of water. When the pressure reading had returned to 10^{-6} m.m. Hg. a Kanthal wound furnace was maneuvered over the glass-silica tube until it was positioned over the silica section and with its hot zone surrounding the gold foil and nickel specimen. Water leads were then connected to commence the flow of the water cooling medium.

When the furnace temperature had become constant at 800°C the flow of water was arrested to allow the nickel surface to become hot. The waxed and soldered joints were kept cool by lengths of lampwick wound around them and soaked with water. After about seven minutes hydrogen was introduced to the chamber to remove the oxide film. The deposition section of the apparatus was isolated from the pumping system by a butterfly valve to allow an adequate pressure of hydrogen to be maintained during deoxidation. This procedure was repeated after which the flow of water was recommenced and the furnace temperature raised to 1100°C .

After 90 minutes at 1100°C , the furnace was cooled and removed. Evacuation was continued together with water cooling until the entire system was cold. The apparatus was then

disassembled to allow the removal of the nickel specimen which had been coated with gold.

At one stage the apparatus used for butt welding ceased to operate effectively as far as the welding of nickel was concerned although other materials e.g. steel, were able to be welded satisfactorily. The reason for this failure lay perhaps in some impurity build up in the nickel which caused an excessive resistance. It was, therefore, decided to replace the welding procedure with silver brazing. Since the brazing material used had a melting point of 720°C , the hydrogen flush had to be carried out at 600°C when most of the heat transmission from the furnace walls was by conduction through hydrogen. This change in procedure resulted in no observable harmful effects.

SECTION 2.ELECTROLYTIC POLISHING OF NICKEL.

After having been machined to the approximate diameter, the nickel cylinder was polished to its final dimension by a No. 400 and then a No. 600 emery paper. A final polishing could not be performed until after the welding operations because the heat then produced caused oxidation of the nickel surface. After welding, any oxide film present was removed with a No. 600 paper.

It was considered inadvisable to polish the nickel with diamond paste because such an operation causes local melting of the surface atomic layers resulting in the formation of a Bickby amorphous layer. Therefore, the final polished surface had to be attained by electrolytic means. The apparatus used shown in fig. 3 enabled the nickel to be polished in situ.

The electrolyte used was a 2:1 mixture of methyl alcohol and nitric acid for which there is no fixed optimum current density and voltage.³⁰ These requirements must be ^{were determined} determined by experiment. The appropriate conditions ^{by a}

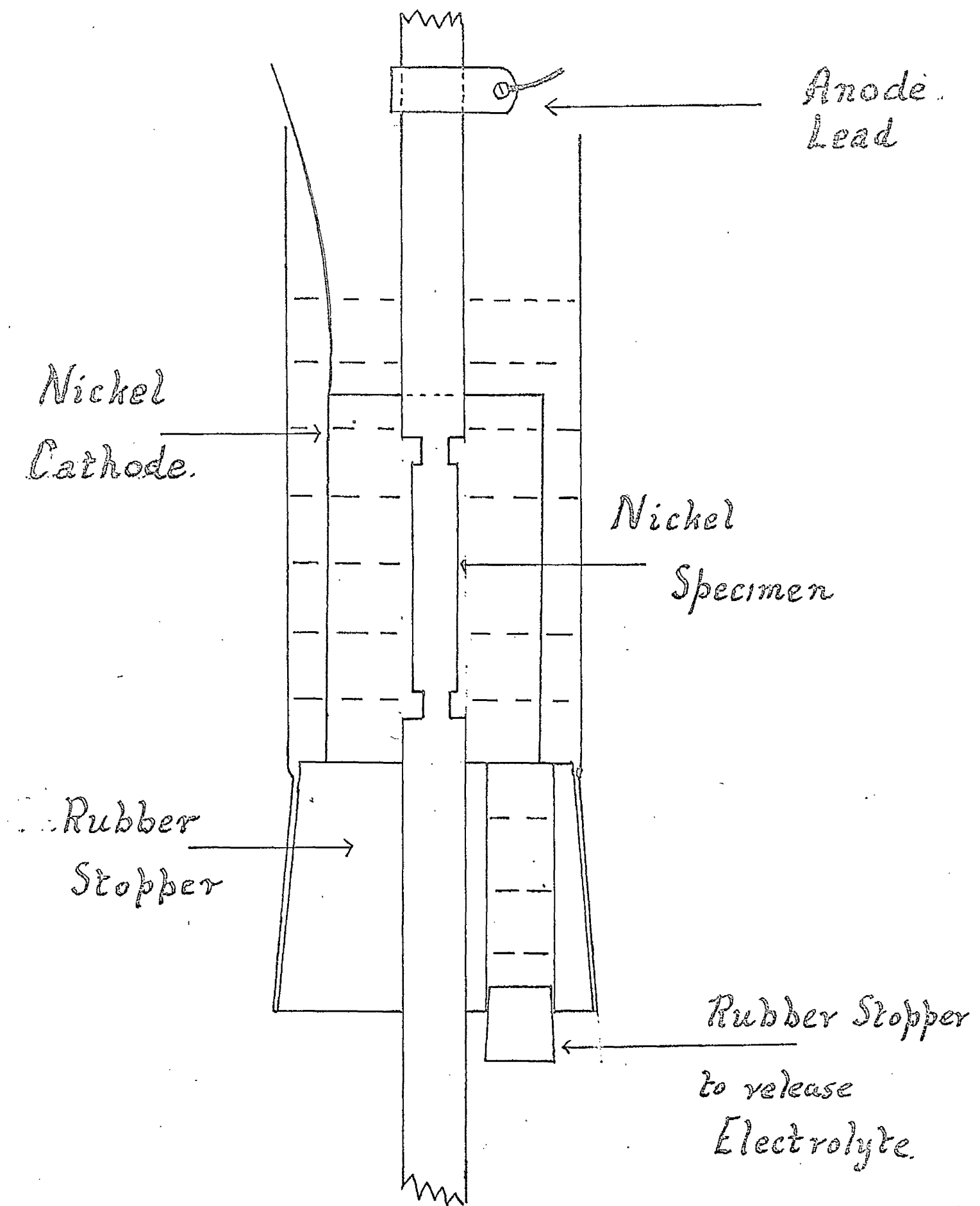


Fig. 3. Apparatus for Electrolytic Polish.

series of trial polishings of nickel cylinders.

From one nickel cylinder 4 cms. in length, two specimens for diffusion studies were obtained. The electrolyte used was a high resistance solution which required a greater energy input to effect polishing than could be obtained with available apparatus. This problem was overcome by painting one half of the cylinder with "Lacomit" protecting fluid which was completely passive to the electrolyte. Sufficient power was available to polish the remainder of the specimen.

When the required voltage was being registered the electrolyte was poured into the bath. After fifteen seconds, the power input was ceased and the rubber stopper was removed to cause a rapid outflow of electrolyte. Water was then immediately used to wash from the nickel surface ^{of} any adhering electrolyte which would otherwise have caused etching.

SECTION 3.DIFFUSION ANNEALS.

The cylinders to be annealed were sealed in evacuated
 -6
 (10 mm.Hg) silica tubes. In order to prevent any physical contact between the gold covered surface and the silica which would have removed some of the gold, the specimen was positioned on a rod of small diameter silica (0.3 cms.) which had been fused centrally in the tubes.

Furnaces with kanthal windings were constructed to give a hot zone ± 0 (-6 C) of length 2.5 cms. Stainless steel tubes of a diameter just less than that of the furnace tubes were inserted to improve the hot zone. This addition enabled the temperature variation of the hot zone to be reduced to ± 0 -0.5 C.

The hot zone temperature was controlled by a fully proportional controller type RT.3/R supplied by Associated Electrical Industries Ltd. A standard 10 ohm platinum resistance thermometer which forms one arm of a Wheatstone Bridge is the temperature sensing element. The furnace winding, the current to which is controlled by 20 turn helical potentiometer, is another arm. It is the balance of the

Wheatstone Bridge which determines the furnace temperature variation. The controller, therefore, contains a unit which compensates for fluctuations in the mains voltage. A close control of temperature up to 1200 °C is an advantage of this type of controller. By careful use the temperature at the centre of the hot zone was controlled to within ± 0.3 °C.

The depth of layer which can be satisfactorily removed on a lathe is about 10^{-3} inches or 2.5×10^{-3} cms. Tomizuka³¹ suggests that ten points are required for an accurate determination of D which meant a penetration depth of 2.5×10^{-2} cms. The required annealing time was calculated approximately from Shownen³². For an accurate penetration curve to be obtained where D is high (10^{-8} cm²/sec.), the depth of penetration should cover a concentration range of one order of magnitude, i.e.

$$\frac{x^2}{4Dt} = -\ln 10^{-1} = 2.3$$

Where D is low (10^{-11} cm²/sec.), the governing factor for obtaining a precise D value is the difficulty of obtaining accurate counts where the activity is 0.002 of the value at $x = 0$ i.e.

$$\frac{x^2}{4Dt} = -\ln (2 \times 10^{-3}) = 5.5$$

Using D values given by Kurz et al.³³ the required annealing

times were estimated on the basis of a compromise between the number of layers required for a sufficient penetration distance and the suitability of the annealing time necessary to give a penetration of 2.5×10^{-2} cms. For example, to obtain such a penetration at 900°C where $D = 10^{-11}$ $\text{cm}^2/\text{sec.}$, the required annealing time is four weeks whereas seven layers of 2.5×10^{-3} cms. requires only two weeks. The time at which diffusion commenced was taken from ten minutes after the specimens were placed in the furnace to allow the specimens to reach the temperature of the furnace. Since the shortest diffusion anneal was 34 hours, any errors introduced by this correction were minimal. Duplicate specimens were annealed simultaneously in the same furnace. Cylinders were annealed at 900, 950, 1000 and 1050°C .

SECTION 4.DETERMINATION OF THE PENETRATION CURVE.

At the termination of the prescribed annealing time the silica tubes were quenched into cold water. The cylinders were then transferred to a lathe where layers of 2.5×10^{-3} cms. were removed (5×10^{-3} cms. of the cylinder diameter). To eliminate edge effects 5×10^{-2} cms. were removed from both ends of the cylinder. From the paper on which it was collected the powder was transferred to a polythene capsule (fig. 4) which had been cleaned in acetone and weighed. The weight of powder was then determined. Considerable care had to be taken to ensure that neither the surface of the paper nor the capsule were touched by hand because sodium ($t_{1/2} = 12$ hours) picked up from the fingers would later have been irradiated and interfered with an accurate determination of the gold concentration. The capsules were then transferred to polythene bags and irradiated.

The powders were irradiated for 30 minutes in a flux of 10^{12} neutrons/cm²/sec. in the nuclear reactor at the Scottish Nuclear Reactor Research Centre, East Kilbride.

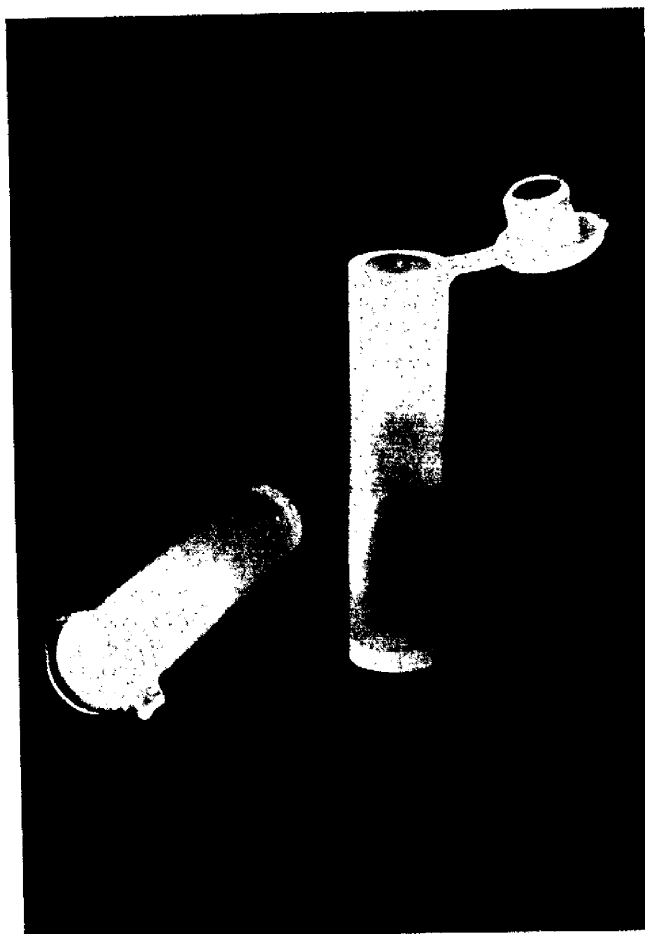


FIG. 4.

POLYTHENE ('ALON') CAPSULES.

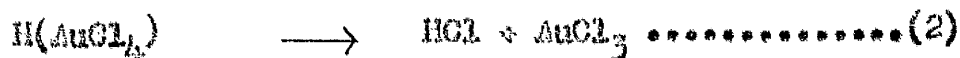
After 25 hours in which to allow the nickel to become inactive, the concentration of gold was determined as the time required for 3×10^3 counts to be recorded on a Geiger-Muller Counter. When the gold concentration became very low the time for 10^3 counts was taken because the time required for 3×10^3 counts was prohibitive. The background count was taken from the summation of three sources.

1. The counts from the end window chamber of the counter i.e. the intrinsic background count for the apparatus.
2. The counts recorded from an empty capsule which had been irradiated along with the powders.
3. The counts obtained from the deactivation of as received pure nickel.

The logarithm of the gold concentration for each layer expressed as the number of counts per 10 mg. of powder per second was plotted against the square of the penetration distance to obtain D. This distance is taken as the mid-point between successive layers.

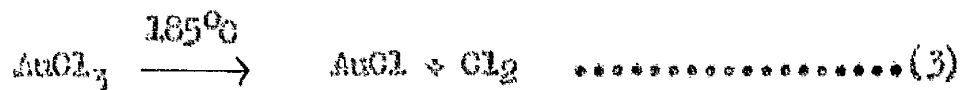
Standard Gold Samples.

Since it was essential to know the order of magnitude of the original gold layer on the nickel surface, some standard gold samples were prepared for comparison. Standard solutions were prepared by first of all dissolving gold in aqua regia.



At this stage some standard solutions were prepared using distilled water.

By subsequent heating AuCl_3 can be decomposed as follows



4 ml. of the most concentrated solution were transferred to a cleaned, dried and weighed silica crucible. The solvent was evaporated off and heating continued to allow reactions (3) and (4) to be effect. A weight of gold was obtained which agreed with the as prepared solution.

Aliquots from each solution were introduced by a syringe into silica quills. The solvent was allowed to evaporate off in a dessicator after which the quills were heated to decompose the gold chloride.

After the quills had been subjected to neutron irradiation it was found that the rates of disintegration were not in proportion to the quantities of gold originally inserted into the quills. Moreover, duplicate samples of each solution were not in agreement. The samples were, therefore, inspected using a "Laben" multi channel pulse height analyser. Considerable activity was recorded of materials other than gold, most certainly caused by impurities present in the silica. Hence, a new method was devised of preparing standards.

A polythene bottle (fig. 5) the neck of which had been heated and drawn out was filled with standard solution and weighed. A small volume of solution was dropped onto a 1 in.² piece of 'Melinex' material which had been previously cleaned with pure ethyl alcohol. The bottle was then re-weighed to determine the weight of solution removed. 'Melinex' is an organic polymer with minimal quantities of impurity (mainly arsenic) because a very low level of catalysts is used in its preparation. To remove the water, the Melinex was heated on a hot plate and an infra red 250 watt lamp was shone on it from above.



FIG. 5.

POLYTHENE BOTTLE FOR THE PREPARATION OF STANDARD GOLD SAMPLES.

When only the solute remained visible the 'Melinex' was folded and placed in a polythene bag to be irradiated. After irradiation the standards were not counted for 25 hours. As explained previously, the nickel powders were not counted until 25 hours after irradiation. Thus to gain some comparison between standards and diffusion specimens, the standards were not counted for 25 hours. The counts recorded from standards of the order of 10^{-5} , 10^{-7} grams were in proportion to each other and to their duplicates.

SECTION 5.PREPARATION OF SINGLE CRYSTALS.

Single crystals of nickel were required for diffusion studies and an attempt was made to grow such crystals. The method basically involved the passing of nickel through the hot zone of a furnace held at 1500°C. The apparatus used is shown in fig. 5. In order to eliminate any oxidation of the melt, it would have been more satisfactory to have produced single crystals under vacuum. Such a procedure, however, would have necessitated the construction of somewhat complicated apparatus and so it was decided that the crystals be grown under an argon atmosphere. A positive pressure of argon was maintained during the crystal growing operation by passing the effluent gas through a constant head of water.

High purity nickel sufficient in quantity to solidify as a crystal of 1 cm. diameter and 4 cms. long was placed in a specially constructed silica tube. This tube was tapered to a point by heating in a hydrogen-oxygen flame. As the melt was lowered through and below the hot zone to where the temperature was 1453°C, solidification

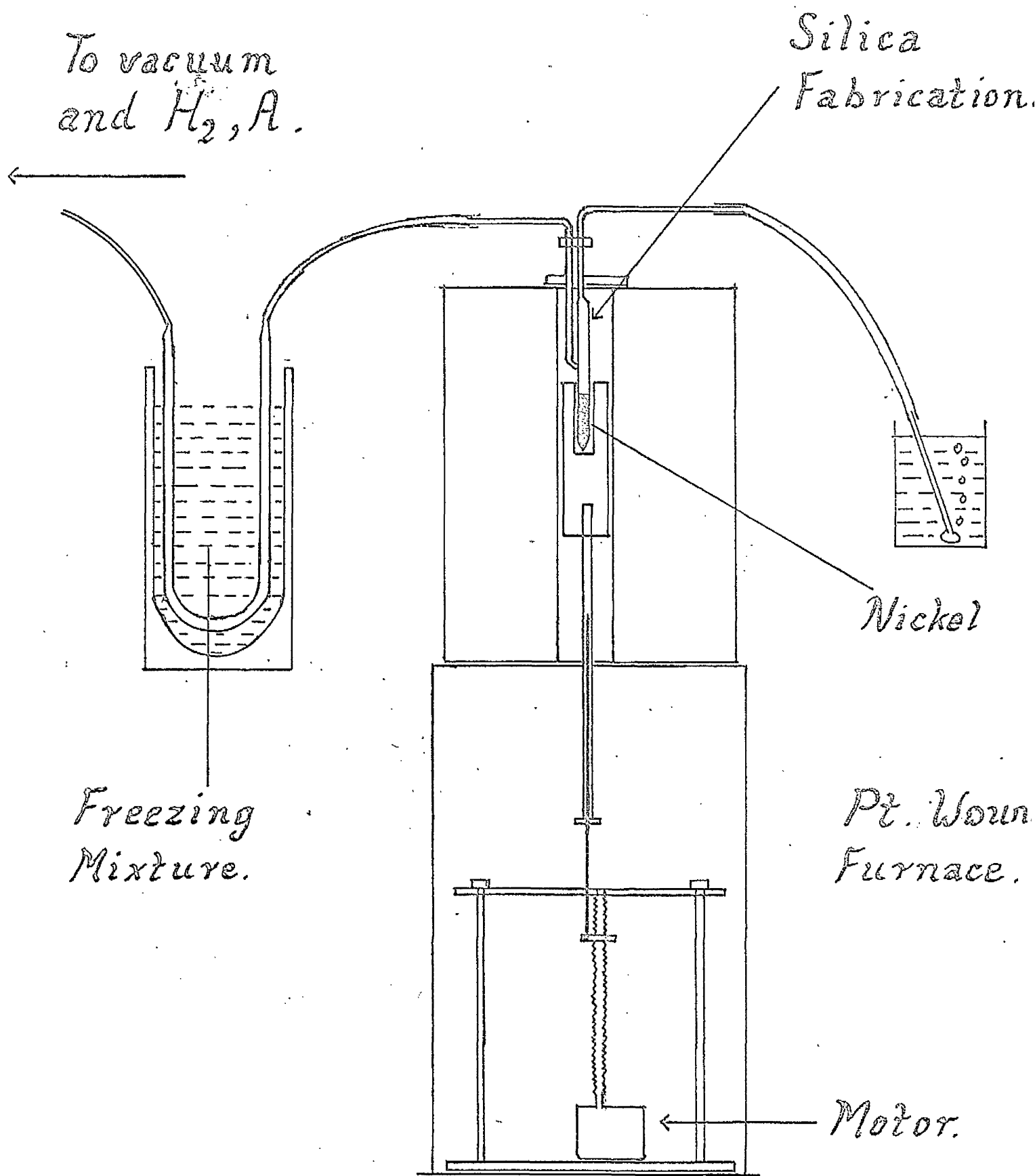


Fig. 6. Apparatus for Growing Single Crystals.

would start at this point to give initially a very small single crystal which would act as a seed from which the entire melt would grow on solidification into a single crystal. Since, at all times, the metal was molten above the growing single crystal, no nucleation could take place and hence no separate grains could be formed. The downward movement of the melt (0.67 cms/hour) was effected by a gearing of threaded brass rod fitted to a motor.

The initial stages of procedure were to seal off the gas outlet tube, evacuate the system down to 10^{-6} mm.Hg, flush consecutively with hydrogen and argon by means of a three-way vacuum stopcock and re-evacuate. When the nickel had reached 800°C , hydrogen was temporarily introduced to clean any oxide from the nickel. After the system had been re-evacuated a steady flow of argon was passed through the melting chamber. Any water vapour or other impurities in the gas were reduced in quantity by passing it through a 'U' tube immersed in a freezing mixture of ethyl alcohol and solid carbon dioxide. The nickel was then raised to 1500°C and the growing operation was commenced.

At the end of the experiment, it was found that the silica tube had become chemically combined to the alumina crucible and could not be removed without fracture. This difficulty was overcome by winding some platinum wire around the silica to prevent any physical contact with the alumina.

This procedure did not meet with any success. The best achievement was an ingot in which there were 6 - 8 grains. Failure to grow single crystals was attributed to vibrations from three sources.

1. The apparatus was positioned on a wooden floor which does not absorb vibrations caused by external forces.
2. The high temperatures required for melting caused the silica gas inlet and outlet tubes of the melting chamber to become slightly fluid and bend causing the silica to rub against the port at the top end of the furnace.
3. As the melt was lowered, a drag was effected by the rubber tubing through which the argon passed.

It was observed, moreover, that the bottom of the silica tube became devitrified because of the length of time (9 - 10 hours) that it was held above 1400°C. This factor resulted in some cracking of the silica tube and oxidation of the ingot.

With a view to eliminating the above drawbacks of vibration and oxidation, a new technique was evolved which used the same drive mechanism as before. The nickel was held in an open silica tube placed in the alumina crucible. Again, the silica was tapered to a point but in this case, a fine pin hole was left at the point. It was hoped that the seed crystal would be produced from nickel which had become solidified while passing through the pin hole. A large furnace was used so that the entire volume of the furnace tube could be under an argon atmosphere. The driving mechanism was sited on a stone floor.

Once again, failure was reported because the lightness of the drive construction did not facilitate a smooth downward passage of the melt.

On account of these failures, the attempt to grow single crystals was abandoned and single crystals were obtained from Metals Research Ltd., Cambridge.

CHAPTER 4

CHAPTER 4

RESULTS AND DISCUSSION

The values of D , D_0 , and Q obtained in the present investigation are shown in Table I. There is a large difference between the present and the previously reported ³³ D values which were obtained by an autoradiographic technique. Although the present results must be considered cautiously because of contamination of the nickel which prevented a rigorous determination of the true gold content of the sections removed from the annealed nickel cylinders, considerable doubt already exists on the validity of the previous work. ³³

Figure 7 shows the variation of the logarithm of the gold concentration with the square of the penetration distance at 900°C. The form of the variation is different from that which is to be expected from the mathematical analysis which is considered to apply in the present case. The successive sections were removed by the same file cleaned between sectioning operations and it was felt that the file might have caused the carry over of gold from one section to the next resulting in this seemingly exponential decrease of $\log_{10} C$. A specimen annealed at 1050°C showed a similar variation. (fig. 8). A new (clean) file was used for ^{each} ^{of} section a second specimen which had been annealed at 900°C. However, as fig. 7 shows, the analysis of penetration yielded a curve which was almost a replica of the previous one. This proves that relative contamination of gold from the filing operation do not account for the form of figs. 7 and 8 (polycrystalline nickel).

TABLE I

SELF-DIFFUSION OF GOLD IN NICKEL

<u>Temp.</u>	<u>Time of Anneal</u> <u>Hrs.</u>	<u>D (present)</u>	<u>D(Kurtz et al.)</u>
900	336	$3.47 \times 10^{-12} \pm 2\%$	1.1×10^{-11}
950	240	$1.07 \times 10^{-11} \pm 3\%$	5.3×10^{-11}
1000	92	$3.89 \times 10^{-11} \pm 6\%$	1.6×10^{-10}
1050	354	$1.09 \times 10^{-10} \pm 5\%$	4.3×10^{-10}
		<u>Present</u>	<u>Kurtz et al</u>
Activation Energy Q (K cal/mole)		72.74 ± 2.54	65.00
Frequency factor D_0 (cm ² sec)		0.01	2.0

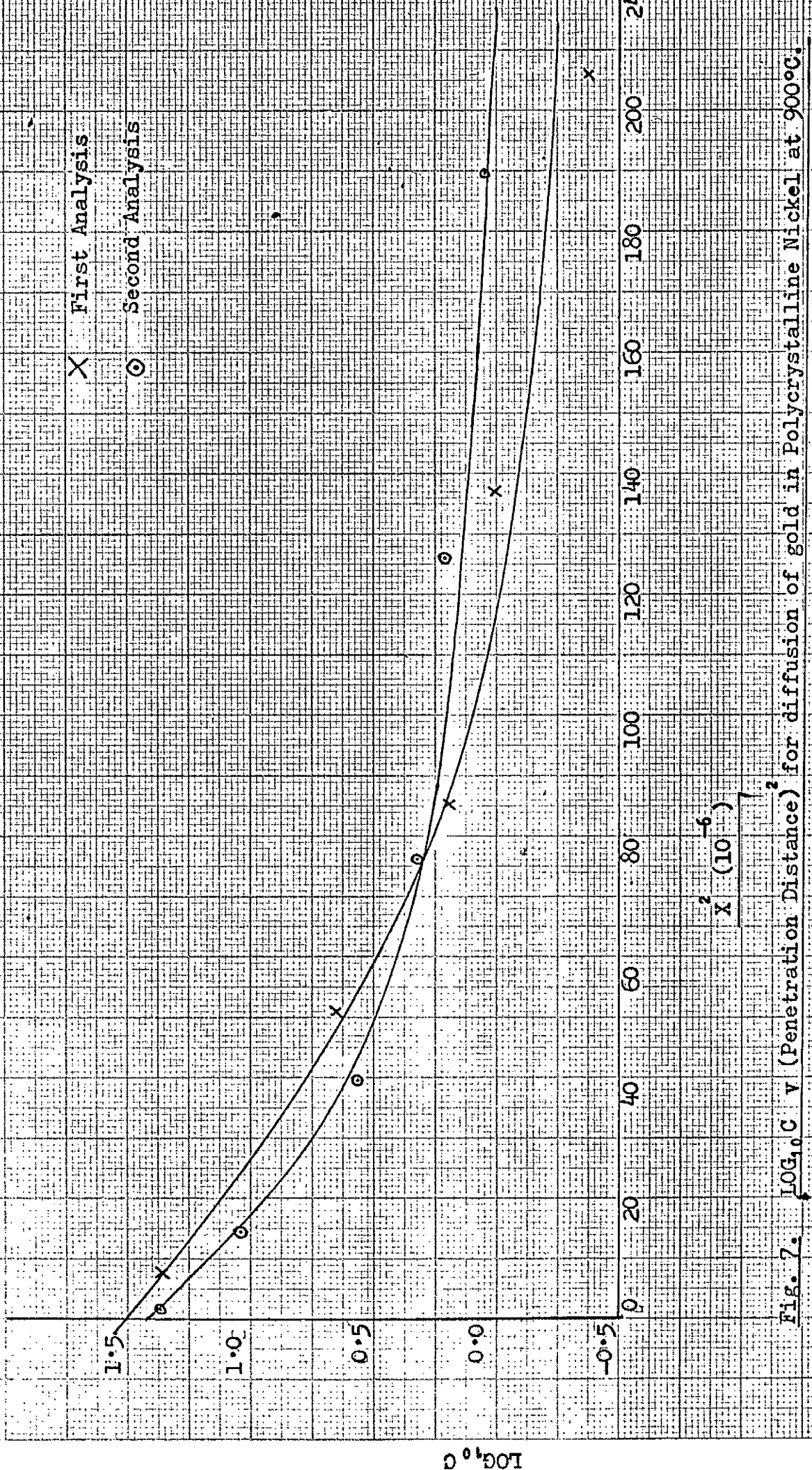


Fig. 7. $\text{LOG}_{10} C v (\text{Penetration Distance})^2$ for diffusion of gold in Polycrystalline Nickel at 900°C .

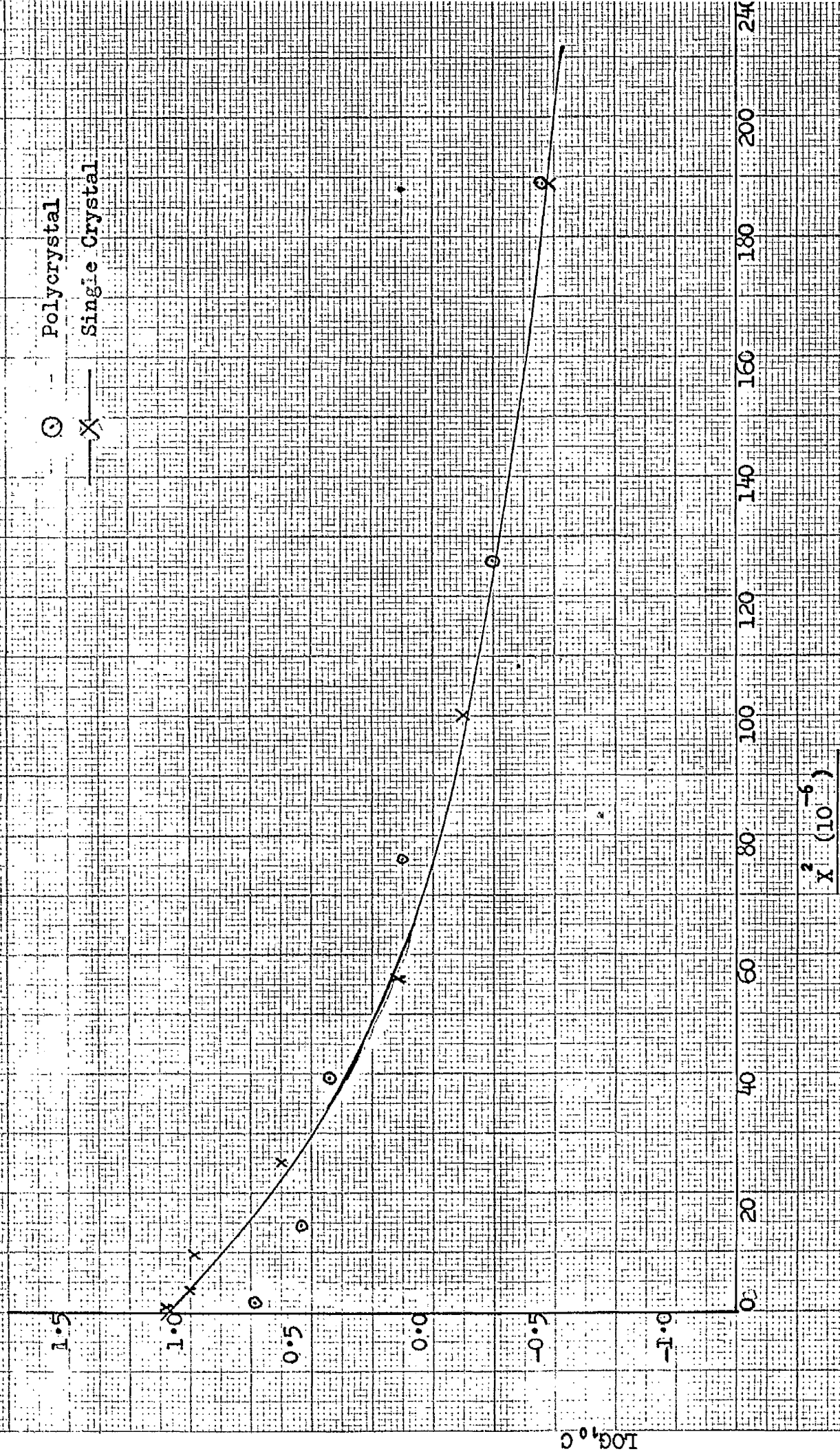


Fig. 8 $\text{Log}_{10} C$ v. (Penetration Distance)² for diffusion of gold in Single and Polycrystalline

Nickel at 1050°C.

A possible explanation of the shape of the graphs is that the thickness of the initial gold layer is in excess of the t required to fulfill the boundary conditions of the problem. Comparison, however, of the summation of the counts over all of the sections (900°C) were compared with standard gold samples irradiated simultaneously indicate that the depth of the original gold layer is $10^2 - 10^3 \text{ \AA}$ which is of the correct order required for the application of the thin film solution.^{33,34}

The form of penetration in the above specimens might readily be explained in terms of (1) grain boundary diffusion being predominant and (2) contamination of the nickel.

It could be contended that the form of the graphs might be explained in terms of an excessive grain boundary diffusion relative to volume diffusion because there is an approximate linear plot over the first few points after which the variation of $\log_{10} C$ with \bar{x}^2 takes the form of a curve. None the less, if such were the case, the value of C would be expected to show a more rapid decrease to zero than is evident from, for example, Table II.

To clarify the question of grain boundary diffusion, a single crystal diffusion specimen was prepared. After having been machined, the single crystal was annealed for twelve hours at 900°C to allow the solution of any small grains formed on the surface as a result of the machining process. A thin film of gold was deposited on this single crystal which was subsequently/

TABLE II

PENETRATION DATA FOR THE SELF-DIFFUSION OF GOLD IN POLYCRYSTALLINE NICKEL

at 1050°C

Time = 1.159×10^5 secs

<u>C(Counts/10 mg/sec)</u>	<u>X(cms x 10⁻³)</u>	<u>log C</u>	<u>X² (cm² x 10⁻⁶)</u>
5.370	1.25	0.7300	1.56
3.543	3.75	0.5483	14.06
2.7476	6.25	0.4389	39.06
1.3403	8.75	0.1271	76.56
0.5386	11.25	-0.2689	126.80
0.3850	13.75	-0.4145	189.06
0.2998	16.25	-0.5230	264.06
0.2558	18.75	-0.5921	351.56
0.3274	21.25	-0.4886	451.56
0.2410	23.75	-0.6180	564.06

TABLE III

PENETRATION DATA FOR CYLINDER OF NICKEL ANNEALED AT 1050°C

Time = 1.159×10^5 secs

<u>Counts/10 mg/sec</u>	<u>x(cms x 10⁻³)</u>
0.293	1.25
0.216	3.75
0.251	6.25
0.203	8.75
0.197	11.25
0.295	13.75
0.223	16.25
0.198	18.75

ly annealed at 1050°C under the same conditions as the polycrystalline specimens. The analysis of the penetration curve was technically unsatisfactory but, as fig. 8 shows, the same levelling out of concentration with penetration distance is evident. This proves that for the depths of penetration in the present investigation the form of figs. 7 and 8 cannot be rationalised in terms of excessive grain boundary diffusion.

From Table II it can be seen that for the last four points the number of counts /10mg/sec. are very nearly equal. Assuming that the proposed mathematical treatment does apply, this equality might be explained in terms of some contamination of the nickel which masks the true gold concentration. Any contaminants in the nickel are irradiated along with the gold and the number of counts subsequently recorded are a summation of the gold contents and of ^{any} this foreign matter of half-life of the same order as that of gold. Table III shows the number of counts obtained from a clean cylinder of nickel which was annealed at 1050°C in the same manner as a gold covered specimen. At all depths the number of counts are approximately equal and that value is almost equal to the counts of the last four sections of the diffusion specimen at 1050°C (Table II). An average value of these counts is 0.25 and when this value is subtracted from all C in Table II, the resultant graph of $\log C \text{ v } x^2$ (fig. 9) is a straight line in keeping with the mathematical analysis of the diffusion problem. This value of 0.25 counts/10 mg/sec. from the blank specimen is higher than the value of 0.11 which was obtained/

2

1

0

-1

-2

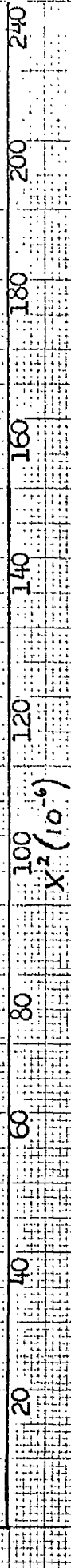


Fig.9. - $\text{LOG}_{10} C v (\text{Penetration Distance})^2$ for diffusion of gold in Polycrystalline Nickel at 10,000°C.

(C has been corrected to take account of the contribution of contamination to the count recorded in radioactivation analysis).

obtained from an irradiated sample of the as received nickel. The only source of the contamination which must account for the extra 0.14 counts is impurities which are transferred in the vapour phase from the commercial pure silica. It is also possible that the effects of this contamination might also mask any logarithmic decay of C as might be expected when grain boundary diffusion is predominant.

One of the samples from the blank nickel was inspected in a "Laben" multichannel pulse height analyser. The graph of the number of counts obtained in each channel is shown in fig. 10. The energies of the gamma photons corresponding to the peaks of the graph are not those corresponding to nickel. An attempt was made to identify the material present but one analysis is not sufficiently rigorous to allow such a determination. Moreover, the peaks could well result from the presence of several elements. As far as can be ascertained, it appears that arsenic, antimony and gallium might be present.

The time available for the present investigation was too limited to allow for the annealing of blank nickel specimens at 900, 950 and 1050°C. For the specimen in which gold was diffused at 1050°C, it has been shown that the value of C at which $\frac{d \log C}{d(x)^2}$ becomes effectively zero is equivalent to the number of counts due to contamination. It was, therefore, decided that for the other temperatures the concentration at which $\frac{d \log C}{d(x)^2} = 0$ should be subtracted from the recorded concentration of each layer. The plots of $\log C \text{ v } x^2$ thus obtained are shown in fig. 11 and the values of D are obtained from the slopes ($= 0.4343/4Dt$) of these graphs. At 900°C, there is yet non-linearity at deeper penetration levels and this might be explained

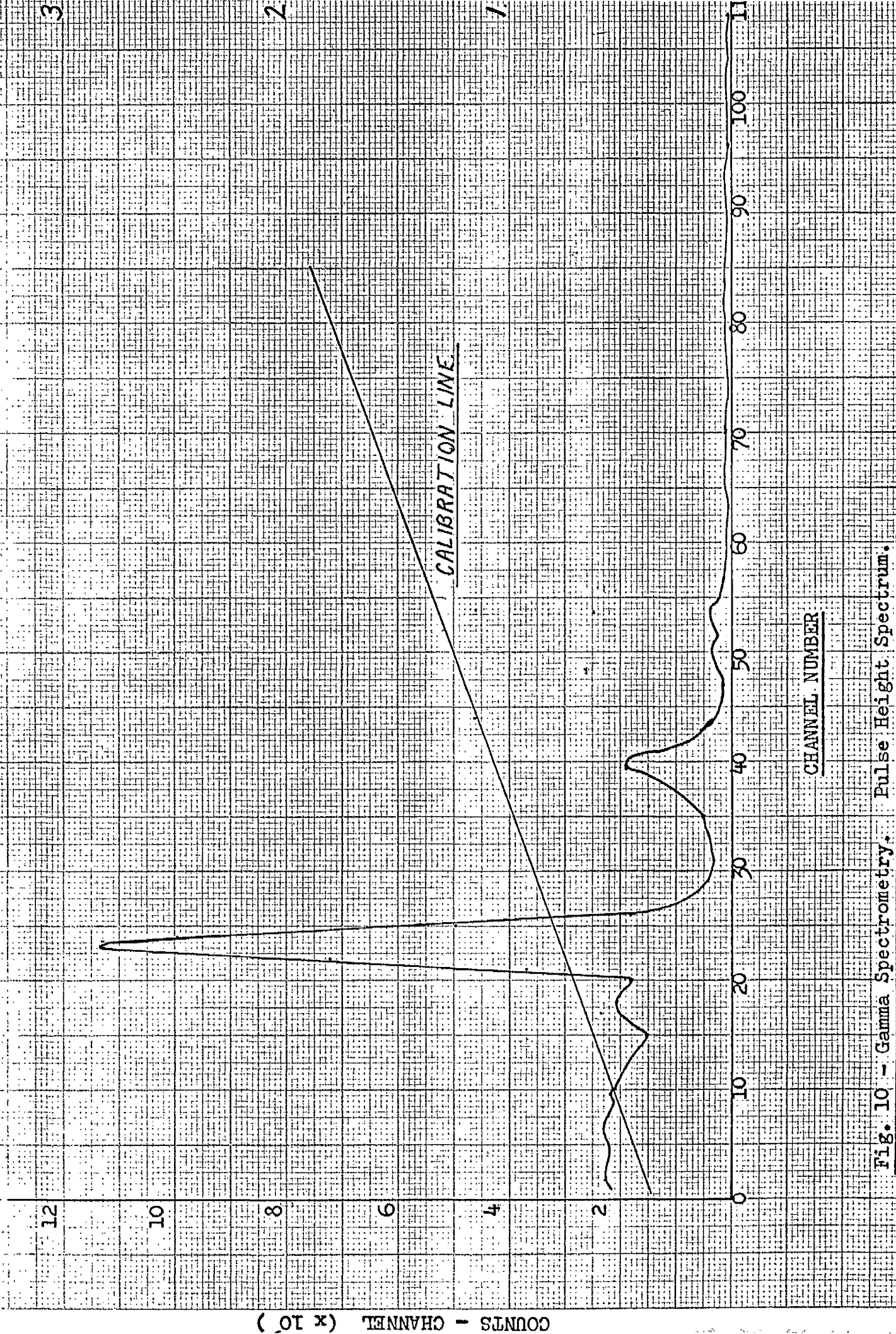


Fig. 10 - Gamma Spectrometry. Pulse Height Spectrum.

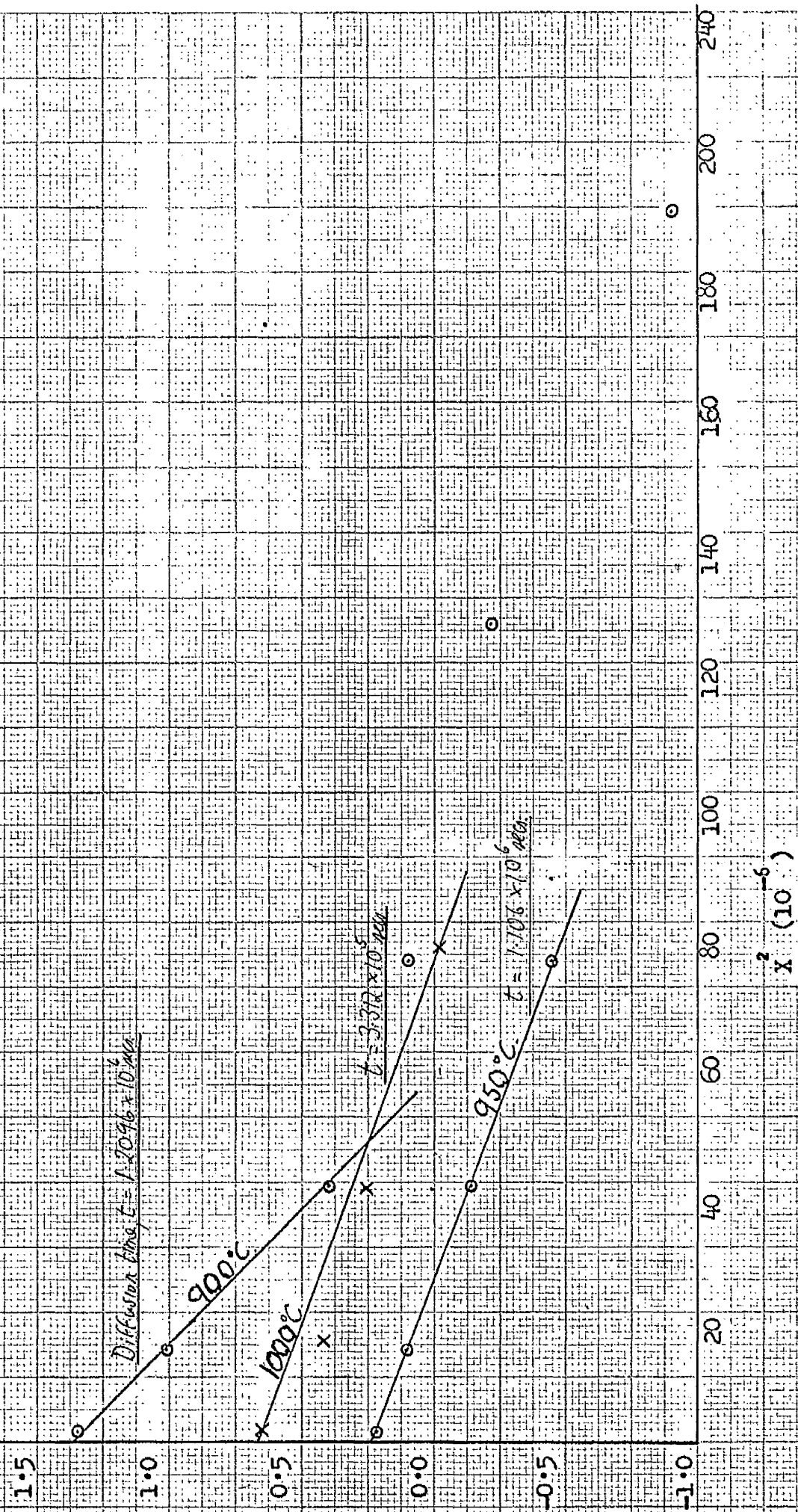


Fig. 11 - $\log_{10} C v$ (Penetration Distance)² for diffusion of gold in Polycrystalline Nickel.

(C has been corrected to take account of the contribution of contamination to the count recorded in radioactivation analysis).

in terms of grain boundary diffusion.

It is most unlikely that during the distillation of gold that the nickel surface was sufficiently cool to be of a temperature comparable to room temperature. The basis of the present method of gold deposition is that the surface of the nickel is so cold that any diffusion of gold is prevented. To confirm this contention, the gold from one cylinder was removed after deposition by rubbing with cotton wool and the surface cleaned of any remaining gold by dipping in cyanide solution. Three layers of 2.5×10^{-3} cms. were removed from this specimen and irradiated. The counts obtained are of the same order as those of the blank specimen and annealed at 1050°C but greater than those obtained from the as received nickel. From this observation it may be inferred:-

- (1) that during distillation some contaminants must reach the nickel surface from the silica section of the deposition chamber and from the silica sleeves.
- (2) that the nickel surface is sufficiently cold to prevent the diffusion of gold as an instantaneous source, but not cool enough to prevent the inward movement of impurities which must certainly, therefore, diffuse rapidly by an interstitial mechanism.

The maximum low pressure reading obtainable with the pump system is 10^{-5} mm. Hg. The best vacuum obtained at distillation temperature was 10^{-5} mm. Hg. This loss of vacuum must be accounted for by/

by the presence of vapour from the materials in the chamber e.g. Na or K ions from the silica.

This rapid interstitial diffusion can account for the equality of concentration in the successive layers as shown in Table III. At 1050°C the diffusion rate is so high that there is no concentration build up at the surface.

Thus by performing sectioning and irradiation of annealed (zero gold content) nickel and of nickel (gold removed) it has been shown that contaminants are present which interfere with any determination of the true gold contents of diffusion specimens.

COUNTING ERRORS

The statistical treatment of the errors involved in the recording of counts from radioactive tracers are considered in standard works.^{35,36} For a Poisson distribution the standard deviation σ is given by

$$\sigma = (N)^{\frac{1}{2}}$$

where N is the number of counts recorded. The larger the number of counts the smaller is the percentage error. Since radioactivity is a statistical phenomenon one count is a good approximation from which the standard deviation can be calculated.

If A_T is the activity (counts/10 mg./sec. in the present case) and A_B is the background count determined from four readings, the standard deviation in the activity of the sample A_S is

$$\sigma_s = \left(\frac{A_T}{t_T} + \frac{A_B}{t_B} \right)^{\frac{1}{2}}$$

where/

where t_T and t_p are the times taken for the recorded number of counts. The application of this standard deviation to the counts recorded from the annealed specimens does not effectively alter the value of C or $\log C$. In the case of the blank nickel specimen, statistical counting errors are insufficient to account for the variation in the number of counts/10 mg./sec. It is quite possible that this variation can be accounted for by contamination which accumulates during the sectioning and weighing operations.

COMPARISON of RESULTS:

A comparison of the results of the present investigation with those of Kurtz et al.³³ is justified only in the case of the D_e value at 1050°C. This result was obtained after a very rigorous analysis of the errors arising from contamination. Kurtz et al.³³ report a diffusion rate which is four times as great as the present value. The method of the former investigations is open to criticism on two points:

- (1) The results reported are for diffusion of a thin film sited in the middle of an infinite bar. Radioactive gold was evaporated on to a disc of nickel and the second disc was welded to this one. The welds were achieved under an argon atmosphere by heating at 850°C under external pressure for one hour. Under these conditions some solution of gold must take place and, therefore, strictly speaking, the boundary conditions of the diffusion problem are not fulfilled.

(2)/

- (2) The penetration profile was obtained by the autoradiographic method. It has been pointed out that this technique is not sufficiently accurate for obtaining satisfactory D values and can only give a good indication of the order of D .³¹

The present results are probably not reliable for several reasons:—

- (1) Grain boundary diffusion cannot be entirely ruled out as no steps were taken to ensure that the grain size was sufficiently large. Microexamination of the nickel revealed a fine grain structure. The predominance of grain boundary diffusion causes a diminution of calculated D values relative to instances where volume diffusion alone is operative.
- (2) A layer of 2.5×10^{-3} cms. taken from one of the diffusion specimens should have a weight of 127 mg. In most instances the weight collected was 0.75 of this quantity. This loss of powder can occur only in the filing operations either as dust or as material retained in the file. It is, therefore, possible that the determined gold concentration is not the true average concentration of the layer.
- (3) It has been concluded that contaminants are introduced into the nickel and that these diffuse probably by an interstitial mechanism. The atom movements involved must cause some strain in the lattice which acts as a barrier to the movement of vacancies and gold atoms and can consequently reduce the rate of diffusion of gold.

Further/

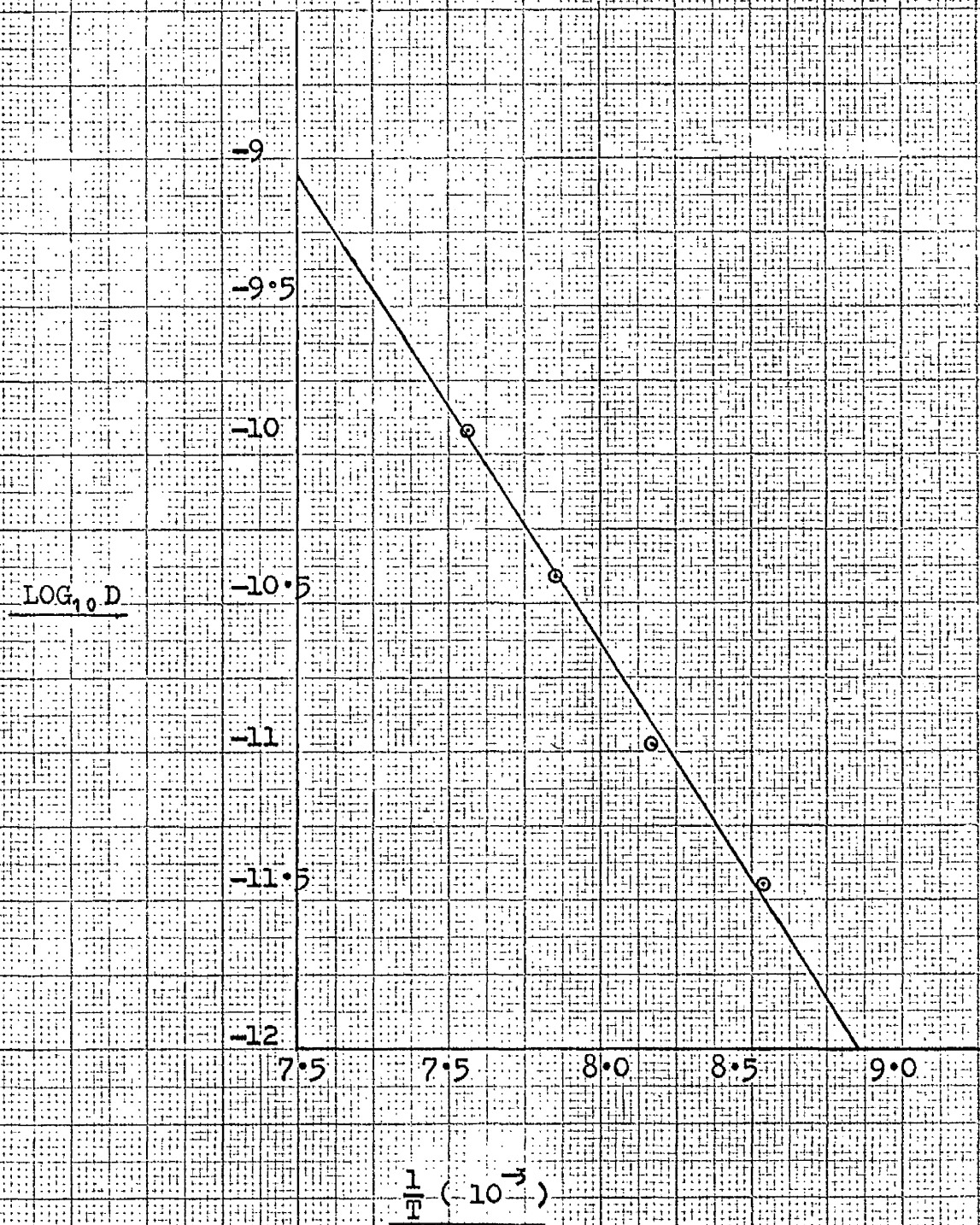


Fig. 12 - $\text{LOG}_{10} D$ - v $\frac{1}{T}$ for diffusion of gold in Polycrystalline Nickel

Further more rigorous work is essential using the present technique before any positive interpretation may be made of the D values obtained.

It is interesting to note that the plot of $\log D \text{ v } 1/T$ shown in fig. 12 gives a satisfactory straight line relationship. An accurate determination of the activation energy is possible in this case. The value obtained (see Table I) is higher than that of previous work.³³ If further work, using the present technique, can verify the activation energy of the present work then some serious reappraisal of the work of Kurtz et al³³ is necessary.

It is important to note that since a good straight line relationship for the activation energy determination is observed by the present results for diffusion coefficients, that these results must have some real significance. Some activation process or barrier to diffusion must exist since it is found that increases of diffusion rate with temperature are consistent with a $\log D \text{ v } \frac{1}{T}$ plot .

CONCLUSION.

The results obtained in the present investigation differ considerably from those of previous work and an attempt has been made to account for these differences. A profile has been obtained from a blank nickel specimen and shows that considerable contamination is present as a result of the manner of experimentation. That the graph of $\log C \text{ v } x^2$ at 1050°C does show a satisfactory linear relationship vindicates the basic premise that in the present case radial effects may be ignored in the mathematical analysis. Thus for diffusion of a thin film of solute into a cylinder of solvent, then provided that the penetration distance is small relative to the radius, it has been shown that the cylinder acts in effect as a semi-infinite slab. In the present series of experiments the penetration distance was 2% of the radius.

The overall usefulness of the present investigation lies in the establishment of a new experimental technique for studying diffusion rates when the solute acts as an instantaneous source. This technique allows the layers of penetration to be removed by a simpler and less laborious means than had been previously been the case. The thicknesses of successive layers can be determined quite simply by using a standard bench micrometer. To machine sections from planes parallel to the endface of a cylinder requires relatively complicated and expensive equipment. Moreover, the thickness of each layer must be determined by weighing the material removed and dividing by the density to/

to obtain the volume of the layer.

The application of the present technique offers a simple method whereby knowledge of the mechanism of impurity diffusion in metals can be obtained. However, if future similar investigations are to prove fruitful, several alterations must be made in the experimental procedure described in chapter 3.

ANALYSIS of the PENETRATION CURVE.

Radioactive analysis has proved so sensitive that steps must be taken to eliminate contamination:-

- (1) All of the commercially pure silica used either in the distillation apparatus or in diffusion anneals should be replaced by very high purity material. In this way the problem of contamination of the diffusion specimens ~~that~~ could be largely overcome. To confirm this view cylinders of nickel could be annealed for various times and any differences in the number of counts relative to annealing time could be ascertained.
- (2) The general environmental conditions under which the samples for analysis were prepared, are unsatisfactory for the accurate determination of the specified solute concentration. Despite great care taken by the present investigator, it has been shown that some contamination resulted during the sectioning and weighing operations. Future work should, therefore, be carried out under very clean laboratory conditions, and with equipment used solely for this type of work.¹

Minor experimental improvements in the experimental method of gold deposition are to be recommended:-

- (1) A platinum wound furnace should replace the Kanthal wound furnace.
A Kanthal wound furnace must remain at a constantly high temperature otherwise recrystallisation of the winding takes place on cooling. Therefore, it was required that the furnace be positioned over, and removed from, the distillation chamber while the latter was under high vacuum.
- (2) The vacuum stopcock should be removed as far as possible from the heat transferred from the furnace, otherwise the vacuum grease tends to melt.
- (3) A system of cooling coils should be manufactured to surround the waxed and soldered joints. The present method is effective in practice but aesthetically unsatisfactory.

ACKNOWLEDGEMENT
ACKNOWLEDGEMENT

I am indebted to Dr. D.J. Fabian, who has supervised this research and whose enthusiasm has been a source of inspiration. To Professor E.C. Ellwood, I am grateful for his advice on many aspects of this investigation.

I also express my gratitude to Mr. G. Grey and his staff for their assistance and advice on the technical aspects of this investigation and especially to Mr. Grey for his assistance on the diffusion studies.

To enable me to carry out this research a grant was given by the Department of Scientific and Industrial Research to which I am grateful.

A.F. Crawley.

REFERENCES

PART I

1. M. Levin. Zeit. Anorg. Chem. 45 (1905) 238.
2. P. De Cesaris. Gazz. Chim. Ital. 43(2) (1913) 609.
3. W. Fraenkel and A. Stern. Zeit. Anorg. Chem. 151 (1926) 105.
4. H. Hafner. Dissertation. Freiburg i. Se., Germany (1927).
5. W. Fraenkel and A. Stern. Zeit. Anorg. Chem. 166 (1927) 161.
6. W. Koster and W. Dannohl. Zeit. Metallkunde. 28 1936 248.
7. A. Munster and K. Sagel. Zeit. Physik. Chem. 14 (1958). 296
8. G. Grube and F. Vaupel. Zeit. Physik. Chem. (1931) B 187.
9. W. Gerloch. Zeit. Metallkunde 22 (1937) 102.
10. O. Kubaschewski and A. Ebert. Zeit. Elektrochem 50 (1944) 138.
11. E. C. Ellwood and K. E. Bagley. Jnl. of Inst. of Metals 80 (1952) 617.
12. G. F. Day. Jnl. of Inst. of Metals 89 (1961) 296.
13. A. Siegle, M. Cohen and B. L. Averbach. Trans. A.I.M.E. 4 (1950) 1320.
14. P. A. Flinn, B.L. Averbach and M. Cohen. Acta. Met. 1 (1953) 664.
15. Y. Tagaki. Proc. Phys-Math. Soc. Japan 23 (1941) 44.
16. B. L. Averbach, A. Flinn and M. Cohen. Acta Met 2 (1954) 92.
17. R. A. Orrani. Acta Met. 3 (1955) 232.
18. L. Vegard. Zeit, Physik 5 (1921) 17.
19. Ya E. Geguzin and B. Ya Pines. Doklady Acad Nauk S.S.S.R. 75 (1950) 387.
20. A. Munster and K. Sagel. National Physical Laboratory. Symposium No. 9.
(1958) Paper 2D.

21. G. Nagorsen and B.L. Averbach. Jnl. of Appl. Phys. 32 (1961) 688.
22. C. M. Sellars and F. Maak. U.S. Dept. Com. Office of Technical Service A.D. 278 068 (1962) 9.
23. R. A. Rapp and F. Mack. Acta Met 10 (1962) 63.
24. T. Houmann. Zeit. Metallkunde 42 (1951) 181.
25. H. B. Huntington and F. Seitz. Phys. Rev. 61(2) 1942 365.
26. R. Simmons and R. Balluffi. Phys. Rev. 119 (1960) 600.
27. A. J. Bradley and A. Taylor. Proc. Roy. Soc. A159 (1937) 56.
28. H. Lipsen and A. Taylor. Proc. Roy. Soc. A 173 (1932) 232.
29. A. J. Bradley and G. G. Seeger. Jnl. Inst. of Metals 64 (1939) 361.
30. A. J. Bradley and H. J. Goldschmidt. Jnl. Inst. of Metals 65 (1939) 3.
31. H. Jones. Proc. Roy. Soc. A147 (1934) 396.
32. G. V. Raynor. Proc. Roy. Soc. A174 (1940) 457.
33. G. V. Raynor. Proc. Roy. Soc. A180 (1942) 107.
34. W. Hume-Rothery and G.V. Raynor. Proc. Roy. Soc. A177 (1940-41) 27.
35. J. O. Betterton and W. Hume-Rothery. Jnl. of Inst. of Metals 80 (1952) 459.
36. W. Hume-Rothery and G. V. Raynor. Proc. Roy. Soc. A174 (1940) 471.
37. E. C. Ellwood. Jnl. of Inst. of Metals 80 (1951) 217.
38. E. C. Ellwood. Jnl. of Inst. of Metals 80 (1951) 605.
39. J. A. Lee and G. V. Raynor. Proc. Phys. Soc. B67 (1954) 737.
40. P. S. Rudman. Acta Met. 10 (1958) 1116.

41. W. J. Helfrich and R. A. Dodd. Trans. Met. Soc. A.I.M.E. 224 (1962) 757.
42. W. J. Helfrich and R. A. Dodd. Acta Met. 11 (1963) 982.
43. W. J. Helfrich and R. A. Dodd. Acta Met. 12 (1964) 667.
44. N. Ridley. Jnl. of Inst. of Metals 92 (1963-64) 123.
45. A. J. Bradley and A. H. Jay. Proc. Phys. Soc. 44 (1932) 563.
46. A. J. Bradley and A. H. Jay. Proc. Phys. Soc. 45 (1933) 507.
47. J. Weigle. Helv. Phys. Acta. 7 (1934) 46.
48. E. R. Jette and F. Foote. Proc. Cambridge. Phys. Soc. 36 (1940) 485.
49. A. Taylor and N. Sinclair. Proc. Phys. Soc. 57 (1945) 126.
50. J. B. Nelson and D. P. Riley. Proc. Phys. Soc. 57 (1945) 160.
51. O. Kubaschewski and E. Evans. "Metallurgical Thermochemistry"
London, Butterworth - Springer Ltd. (1951).
52. K. Q. Bagley. Ph.D. Thesis, King's College, Newcastle (1951).
53. K. Lonsdale. Acta Cryst. 3 (1950) 400.
54. R. A. Andrievskii. Vopr. Poroshkovoi. Metall., i. Prochn. Materialov.
Kiev Ukrainian Acad. of Science 6 (1958) 29.
55. International Critical Tables of Num. Data Phys. Chem. Tech. 3 29.
56. T. Batuceas and J. Alonso. An. fis y quim. 44B 1101 (1948)
Chem. Abs 43 (1949) 3678g.
57. F. J. Hallow. Phil. Mag. 7 (1929) 674.
58. J. A. Beattie. et al. Proc. Amer. Acad. Arts and Science 74 (1941) 32
59. W. B. Pearson. "Handbook of Lattice Spacings of Metals and Alloys"
Pergamon Press (1956)
60. I. Langmuir. Phys. Rev. 2(3) (1913) 331.

61. E. A. Owen. Jnl. Inst. of Metals 69 (1943) 2.
62. F. Von Batchelder and R. Rachele. Phys. Rev. 105 (1957) 59.

PART II

1. A. Fick "Uber Diffusion", Pogg Ann 94 (1855) 59.
2. H. S. Carslaw and J. C. Jaeger. "Conduction of heat in solids" Oxford University Press Fair Lawn N.J. (1959).
3. J. Crank "Mathematics of Diffusion" Oxford University Press Fairlawn N.J. (1956).
4. C. R. Matano. Japanese Jnl. of Phys. 83 (1933) 109.
5. L. Boltzmann. Ann Physik 53 (1894) 960.
6. F. N. Rhines and R. F. Mehl. Trans. A.I.M.M.E. 128 (1938) 185.
7. A. Smigelskas and E. Kirkendall. Trans. A.I.M.E. 171 (1947) 130.
8. L. S. Darken. Trans A.I.M.E. 174 (1948) 184.
9. L. G. Correa da Silva and R. F. Mehl. Trans A.I.M.E. 191 (1951) 155.
10. C. Zener. Acta Cryst 3 (1950) 346.
11. G. M. Pound, W. R. Bitler and H. W. Paxton. Phil. Mag. (8) 6 (1961) 473.
12. N. H. Nachtreib and G. S. Handler. Acta Met. 2 (1954) 797.
13. F. G. Shewmon. "Diffusion in Solids" McGraw-Hill Book Company (1963) 52.
14. D. Lazarus. Phys. Rev. 93 (1954) 973.
15. R. A. Swalin. Acta Met. 5 (1957) 443.
16. W. C. Mallard and L. M. Slifkin et al. Phys. Rev. 129 (1963) 617.
17. J. Bardeen and C. Herring. "Atom Movements" Amer. Soc. for Metals Cleveland, Ohio (1951) 87.
18. K. Compaan and Y. Haven. Trans. Faraday Soc. 52 (1956) 786.

19. A. D. Le Claire and A. B. Liddiard. *Phil. Mag.* (6) 1 (1956) 518.
20. D. Turnbull. "Atom Movements" Amer. Soc. for Metals Cleveland, Ohio (1951) 129.
21. J. C. Fisher. *Jnl. Appl. Phys.* 22 (1951) 74.
22. R. T. Whipple. *Phil. Mag.* 45 (1954) 1225.
23. E. S. Wajda. *Acta Met.* 2 (1954) 184.
24. J. R. MacEwan, J. U. MacEwan and L. Yaffe. *Canadian Jnl. of Chem* 37 (1959) 1623.
25. R. C. Koch. "Activation Analysis Handbook" Academic Press New York (1960).
26. C. E. Grouthamel. "Applied Gamma-Ray Spectrometry" Pergamon Press (1960)
27. Radio Chemical Manual. Part 1. Physical Data. N.M.S.O. (1962).
28. D. S. Tarnhauser. *Jnl. Appl. Phys.* 27 (1956) 662.
29. J. M. Blakeley and H. Mykura. *Acta Met.* 9 (1961) 570, 595.
30. G. E. Pellissier et al. *Met. Progress* 31 (1940) 554.
31. C. T. Tomizuka. "Methods of Experimental Physics" Academic Press New York 6A (1959)
32. P. G. Shewmon. "Diffusion in Solids". McGraw-Hill Book Company (1963) 10.
33. A. D. Kurtz, B. L. Averbach and M. Cohen. *Acta Met.* 3 (1955) 442.
34. J. E. Reynolds and B. L. Averbach, and M. Cohen. *Acta Met.* 5 (1957) 29.
35. H. Bowen and D. Gibbons "Radioactivation analysis" Clarendon Press 1972.
36. C. Leymonie "Radioactive Tracers in Physical Metallurgy" London: Chapman and Hall 1963, 13.

